UNIVERSITY OF CALIFORNIA, SAN DIEGO
SCRIPPS INSTITUTION OF OCEANOGRAPHY
VISIBILITY LABORATORY
SAN DIEGO, CALIFORNIA 92152

AIRBORNE MEASUREMENTS OF OPTICAL ATMOSPHERIC PROPERTIES, SUMMARY AND REVIEW

Seibert Q. Duntley, Richard W. Johnson, and Jacqueline I. Gordon

CONTRACT NO. F 19628-70-C-0054
Project No. 7621
Task No. 762104
Work Unit No. 76210401

FINAL REPORT
1 November 1969 – 31 August 1972
November 1972

Contract Monitor: Robert W. Fenn, Optical Physics Laboratory

Prepared for

AIR FORCE CAMBRIDGE RESEARCH LABORATORIES
AIR FORCE SYSTEMS COMMAND
UNITED STATES AIR FORCE
BEDFORD, MASSACHUSETTS 01730

Approved

Seibert Q. Duntley

Seibert Q. Duntley, Director
Visibility Laboratory

Approved for Distribution

William A. Nierenberg

William A. Nierenberg, Director
Scripps Institution of Oceanography

ABSTRACT

This report summarizes a 3-year period of collecting optical atmospheric data in the daytime chiefly with airborne instruments. Nine field expeditions were made between November 1969 and August 1972 in various places in the United States and Europe, primarily during the spring and fall. Measurements were made in five spectral regions, as follows: three narrow band optical filters with mean wavelengths of 478, 664, and 765 nanometers, and two broad band sensitivities, one representing the S-20 multiplier phototube incorporating an ultraviolet rejection filter with a mean wavelength of 532 nanometers, the other representing the photopic response with a mean wavelength of 557 nanometers. Optical measurements included total scattering coefficient and sky and terrain radiance. These data were used to calculate natural irradiance on a horizontal plane surface, directional reflectance of terrain, atmospheric beam transmittance, path radiance, and directional path reflectance. The methods of data collection and data processing are reviewed, the resultant data bank described, and initial comparisons made between several of the field expeditions.

SUMMARY

This is the Final Report prepared in compliance with AFCRL Contract F19628-70-C-0054. The principal tasks under this contract were (1) to make an instrument conversion from nighttime to daytime capability and (2) to perform a series of missions to collect atmospheric optical data in various places in the United States and Europe. The purpose of the measurements was to determine several important optical properties of various downward-inclined paths of sight. These properties include the atmospheric beam transmittance, path radiance, path reflectance, background reflectance, background radiance, and contrast transmittance.

Nine field trips were made. Data from the first field trip, which was to southern Germany, and from the second trip to central New Mexico have been issued as Scientific Reports 1 and 2 [Duntley, *et al.* (1972a, 1972b)]. The status of the total data bank resulting from the 3-year period is reviewed in this report.

The instrumentation developed at the Visibility Laboratory and mounted in Air Force C-130A, aircraft No. 50022, consisted of a total scattering meter (or integrating nephelometer) for determining the total scattering coefficient, two sky scanning radiometers for recording upper and lower sky radiances, a dual irradiometer for recording alternately the downwelling and upwelling irradiances upon horizontal plane surfaces, an equilibrium radiance telephotometer, and a variable direction path function meter. The meteorological instrumentation included a Royco particle counter, pressure transducers, a dewpoint hygrometer, and an AN/AMQ-17 aerograph for measuring ambient temperature and humidity.

Each optical instrument was fitted with five optical filters causing it to measure at three narrow band wavelengths of the spectrum and two broad pass bands as follows: three narrow band filters at mean wavelengths of 478, 664, and 765 nanometers, a filter representing the photopic response with a mean wavelength of 557 nanometers, and one with a mean wavelength of 532 nanometers representing the S-20 multiplier phototube with an ultraviolet rejection filter.

All but the Royco data were recorded on magnetic tape in the aircraft by means of a 42-channel magnetic tape data logger. The data tapes were returned to the Visibility Laboratory to be processed using the computer facilities at the University of California, San Diego.

A ground-based station near each flight track contained effectively duplicate instrumentation for obtaining optical data. In addition, for all but the first field trip, it contained a contrast reduction meter for measuring earth-to-space beam transmittance and path radiance.

CONTENTS

LIST OF ILLUSTRATIONS

RELATED CONTRACTS AND PUBLICATIONS

Related Contracts: None

Publications:

S. Q. Duntley, R. W. Johnson, and J. I. Gordon, "Airborne Measurements of Optical Atmospheric Properties in Southern Germany," AFCRL-72-0255, SIO Ref. 72-64 (July 1972).

S. Q. Duntley, R. W. Johnson, and J. I. Gordon, "Airborne and Ground-Based Measurements of Optical Atmospheric Properties in Central New Mexico," AFCRL-72-0461, SIO Ref. 72-71 (September 1972).

J. I. Gordon, J. L. Harris, Sr., and S. Q. Duntley, "Method of Measuring Earth-to-Space Contrast Transmittance from Ground Stations," submitted to Applied Optics on 21 September 1972.

GLOSSARY AND NOTATION

The notation used in reports and journal articles produced by the Visibility Laboratory staff follow, in general, the rules set forth in pages 499 and 500, Duntley *et al* (1957). These rules are:

Each optical property is indicated by a basic (parent) symbol.

A presubscript may be used with the parent symbol as an identifier, e.g., b indicates background while t denotes an object.

A postsubscript may be used to indicate the length of a path of sight, e.g., r denotes an *apparent* property as measured at the end of a path of sight of length r, while o denotes an *inherent* property based on the hypothetical concept of a photometer located at zero distance from an object.

A postsuperscript *, or a postsubscript$_*$, is employed as a mnemonic symbol signifying that the radiometric quantity has been generated by the scattering of ambient light reaching the path from all directions.

The parenthetical attachments to the parent symbol denote altitude and direction. The letter z indicates altitude in general; z_t is used to specify the altitude of an object. The direction of a path of sight is specified by the zenith angle θ and the azimuth ϕ. In the case of irradiances, the downwelling irradiance is designated by d, the upwelling by u.

A(z)	Albedo at altitude z, defined by the equation $A(z) \equiv H(z,u)/H(z,d)$. (*Scalar Albedo*, at altitude z, is the ratio $h(z,u)/h(z,d)$.)
AGL	Above ground level.

$C_o(z_t,\theta,\phi)$ Inherent universal contrast determined for a path of sight of zero length at altitude of the object z_t in the direction of zenith angle θ and azimuth ϕ. This property is defined by the equation

$$C_o(z_t,\theta,\phi) \equiv \frac{{}_tN_o(z_t,\theta,\phi) - {}_bN_o(z_t,\theta,\phi)}{{}_bN_o(z_t,\theta,\phi)} .$$

$C_r(z,\theta,\phi)$ Apparent universal contrast as determined at altitude z from the end of path of sight of length r in the direction of the zenith angle θ and azimuth ϕ. This property is defined by the equation

$$C_r(z,\theta,\phi) \equiv \frac{{}_tN_r(z,\theta,\phi) - {}_bN_r(z,\theta,\phi)}{{}_bN_r(z,\theta,\phi)} .$$

g Acceleration of gravity.

$H(z)$ Scale height at altitude z, the height of a homogeneous atmosphere having the density of the layer at altitude z.

$H(z,d)$ Irradiance produced by downwelling flux as determined on a horizontal flat plate at altitude z. In this report d is used in place of the minus sign in the notation $H(z_t,-)$ which appears in Duntley (1969). This property may be defined by the equation

$$H(z,d) \equiv \int_{2\pi} N(z,\theta',\phi')\cos\theta' \, d\Omega .$$

$H(z,u)$ Irradiance produced by upwelling flux as determined on a horizontal flat plate at altitude z. Here u is substituted for the plus sign formerly used in the notation $H(z,+)$.

$h(z)$ Scalar irradiance. This may be defined as the radiant flux arriving at a point, from all directions about that point, at altitude z (Tyler and Preisendorfer, 1962):

$$h(z) \equiv h(z,d) + h(z,u) .$$

$h(z,d)$ Scalar irradiance produced by downwelling flux. This may be defined as the radiant flux from the upper hemisphere arriving at a point at altitude z.

${}_kh(z,d)$ Scalar irradiance defined as the radiant flux from the upper hemisphere sky (flux from the sun is not included) arriving at a point at altitude z.

${}_sh(z)$ Scalar irradiance defined as the radiant flux from the sun arriving at a point at altitude z.

$h(z,u)$ Scalar irradiance produced by upwelling flux. This may be defined as the radiant flux from the lower hemisphere arriving at a point at altitude z.

$L(z)$ Attenuation length at altitude z. This property is the reciprocal of the attenuation coefficient, that is,

$$L(z) \equiv \alpha(z)^{-1} .$$

$\bar{L}(z)$ Equivalent attenuation length is defined as

$$\bar{L}(z) = \frac{-z}{\ln T_z(0,0)} .$$

$m_\infty(z,\theta)/m_\infty(z,0)$ Relative optical airmass.

$N(z,\theta,\phi)$ Radiance as determined from altitude z in the direction specified by zenith angle θ and azimuth ϕ.

${}_bN_o(z_t,\theta,\phi)$ Inherent background radiance as determined at altitude of the photometer z_t at zenith angle θ and azimuth ϕ.

${}_bN_r(z,\theta,\phi)$ Apparent background radiance as determined at altitude z from the end of a path of sight of length r at zenith angle θ and azimuth ϕ. This property may be defined by the equation

$${}_bN_r(z,\theta,\phi) \equiv {}_bN_o(z_t,\theta,\phi)\, T_r(z,\theta) + N_r^*(z,\theta,\phi) .$$

${}_tN_o(z_t,\theta,\phi)$ Inherent radiance of an object as determined at altitude of the photometer z_t at zenith angle θ and azimuth ϕ.

${}_tN_r(z,\theta,\phi)$ Apparent radiance of an object as determined at altitude z from the end of a path of sight of length r at zenith angle θ and azimuth ϕ. This property may be defined by the equation

$${}_tN_r(z,\theta,\phi) \equiv {}_tN_o(z_t,\theta,\phi)\, T_r(z,\theta) + N_r^*(z,\theta,\phi) .$$

$N_q(z,\theta,\phi)$ Equilibrium radiance at altitude z with the direction of the path of sight specified by zenith angle θ and azimuth ϕ. This property is a point function of position and direction.

$N_*(z,\theta,\phi)$ Path function at altitude z with the direction of the path of sight specified by zenith angle θ and azimuth ϕ. This property is defined by the equation

$$N_*(z,\theta,\phi) \equiv \int_{4\pi} \sigma(z,\beta')\, N(z,\theta',\phi')\, d\Omega .$$

This property also is a point function of position and direction.

$N_r^*(z,\theta,\phi)$ Path radiance as determined at altitude z at the end of a path of sight of length r in the direction specified by zenith angle θ and azimuth ϕ.

$n(z)$ Index of refraction at altitude z.

$P(z)$ Pressure at altitude z.

psia Pressure, absolute, pounds per square inch.

psid Pressure, differential, pounds per square inch.

${}_bR_o(z_t,\theta,\phi)$ Inherent background reflectance as determined at the altitude of an object z_t and viewed at zenith angle θ and azimuth ϕ.

$R_r^*(z,\theta,\phi)$ Directional path reflectance as determined at altitude z at the end of a path of sight of length r in the direction specified by zenith angle θ and azimuth ϕ.

$R_q(z,\theta,\phi)$ Equilibrium reflectance is defined as $R_q(z,\theta,\phi) = N_q(z,\theta,\phi)\,\pi / H(z,d)$.

$R/M(0)$ Universal gas constant.

$\overline{S_\lambda T_\lambda}$ Standardized relative spectral response of filter/cathode combination where S_λ is spectral sensitivity of the multiplier phototube cathode and T_λ is spectral transmittance of optical filter.

$s(z)$ Total volume scattering coefficient as determined at altitude z. This property may be defined by the equation

$$s(z) \equiv \int_{4\pi} \sigma(z,\beta)\, d\Omega \quad .$$

In the absence of atmospheric absorption, the total volume scattering coefficient is numerically equal to the attenuation coefficient.

${}_Ms(z)$ Total volume scattering coefficient for Mie scattering at altitude z.

${}_Rs(z)$ Total volume scattering coefficient for Rayleigh scattering at altitude z.

$T(z)$ Temperature in degrees Kelvin at altitude z.

$T_r(z,\theta)$ Beam transmittance as determined at altitude z for a path of sight of length r at zenith angle θ. This property is independent of azimuth in atmospheres having horizontal uniformity. It is always the same for the designated path of sight or its reciprocal.

${}_b\tau_r(z,\theta,\phi)$ Contrast transmittance as determined at altitude z at the end of a path of sight of length r and specified by zenith angle θ and azimuth ϕ. This property is *not* independent of azimuth and is *not* the same for the designated path of sight and its reciprocal.

W_λ Spectral emittance (power/unit of area) of electromagnetic flux from a plane surface.

$\bar{y}$ Symbol for visual efficiency function.

ZSV Zero scale value. The zero point on the linear scale when the radiometric or photometric quantity x is equal to a reference radiometric or photometric quantity x_o as shown in equation

$$\log [x_o / x] = 0 .$$

z Altitude, usually used as above ground level.

z_t Altitude of an object.

$\alpha(z)$ Volume attenuation coefficient as determined at altitude z. In the absence of atmospheric absorption, the attenuation coefficient is numerically equal to the volume scattering coefficient.

β Symbol for scattering angle of flux from a light source. It is equal to the angle between the line from the source to the observer and the path of sight.

β' Symbol for scattering angle of flux from a discrete part of the sky. It is equal to the angle between the direction specified by θ' and ϕ' and the path of sight.

Δ Symbol to indicate incremental quantity and used with r and z to indicate small, discrete increments in path length r and altitude z.

δ_λ Response area is defined as $\delta_\lambda = \Sigma(\overline{S_\lambda T_\lambda})\, \Delta\lambda$.

ϵ_λ Spectral emissivity of tungsten filament.

ζ Symbol for radius of the earth in Eq. 2-11 and 2-13 and Figure 2-2.

θ Symbol for zenith angle. This symbol is usually used as one of two coordinates to specify the direction of a path of sight.

θ' Symbol for zenith angle usually used as one of two coordinates to specify the direction of a discrete portion of the sky.

λ Symbol for wavelength.

$\bar{\lambda}$ Mean wavelength is defined as $\bar{\lambda} = \Sigma\lambda\, (\overline{S_\lambda T_\lambda})\, \Delta\lambda / \delta\lambda$.

$\rho(z)$ Density at altitude z.

σ Symbol for volume scattering function. Parenthetical symbols may be added; for example, β may be used to designate the scattering angle from a source. In Gordon (1969) the parenthetical symbols are z and β for altitude and scattering angle.

$\sigma(z,\beta)/s(z)$ Proportional directional volume scattering function. This may be defined by the equation

$$\int_{4\pi} [\sigma(z,\beta)/s(z)] \equiv 1 .$$

ϕ Symbol for azimuth. The azimuth is the angle in the horizontal plane of the observer between a fixed point and the path of sight. The fixed point may be, for example, true north, the bearing of the sun, or the bearing of the moon. This symbol is usually used as one of two coordinates to specify the direction of a path of sight.

ϕ' This symbol for azimuth is usually used as one of two coordinates to specify the direction of a discrete portion of the sky.

Ω Symbol for solid angle. For a hemisphere

$$\Omega = 2\pi \text{ steradians;}$$

for a sphere $\Omega = 4\pi$ steradians.

1. INTRODUCTION

This is the final report prepared under Contract F19628-70-C-0054. It discusses activities, accomplishments, and recommendations related to an atmospheric optical properties measurement program conducted during the interval 1 November 1969 through 31 August 1972. The experimental measurement flights made during this contract interval as part of the Visibility Laboratory's ongoing program of environmental documentation are identified in Table 1-1. Selected sets of the resulting measurements have been presented in two preceding reports: AFCRL-72-0255, "Airborne Measurements of Optical Atmospheric Properties in Southern Germany," Duntley, *et al.* (1972a), and AFCRL-72-0461, "Airborne and Ground-Based Measurements of Optical Atmospheric Properties in Central New Mexico," Duntley, *et al.* (1972b). These measurements and the computations related to their use are examples of the Laboratory's continuing development of improved techniques for predicting, by calculation from physical data, the probabilities with which any object can be visually detected and recognized.

The radiometer spectral responses were standardized during this contract interval, as illustrated in Fig. 1-1. They were discussed in detail in Section 3.5 of Duntley, *et al.* (1972a). The only alteration from the specifications discussed in that reference was to change the identification codes associated with each filter. Beginning with Flight C-160, 2 March 1971, the coding for the photopic and near infrared filters was reversed.

Table 1-1

Summary of Airborne Data Collection Flights

Flight No.	Dates	Project Title*	Geographic Location
C-120 to C-144	18 Apr 70 to 7 Jun 70	HAVEN VIEW	Germany, Spain, Morocco
C-150 to C-158	22 Oct 70 to 4 Nov 70	ATOM	Socorro, New Mexico
C-160 to C-167	2 Mar 71 to 16 Mar 71	SNOWBIRD	Green Bay, Wisconsin
C-170 to C-173	29 Mar 71 to 1 Apr 71	LOCAL I	Yuma, Ariz. – San Clemente Is., Cal.
C-175 to C-177	22 Apr 71 to 2 May 71	DRUMMER BOY	Watertown, New York
C-180 to C-188	11 Aug 71 to 24 Aug 71	METRO	St. Louis, Mo.
C-190 to C-191	21 Oct 71 to 27 Oct 71	LOCAL II	Yuma, Ariz. – San Clemente Is., Cal.
C-193 to C-198	25 Jan 72 to 2 Feb 72	LOCAL III	Edwards, Cal., Yuma, Ariz., San Clemente Is., Cal.
C-200 to C-207	12 Apr 72 to 29 Apr 72	SENTRY	Concord, New Hampshire

* Project titles are for procedural identification only and are not necessarily utilized or recognized by agencies or organizations outside the Visibility Laboratory.

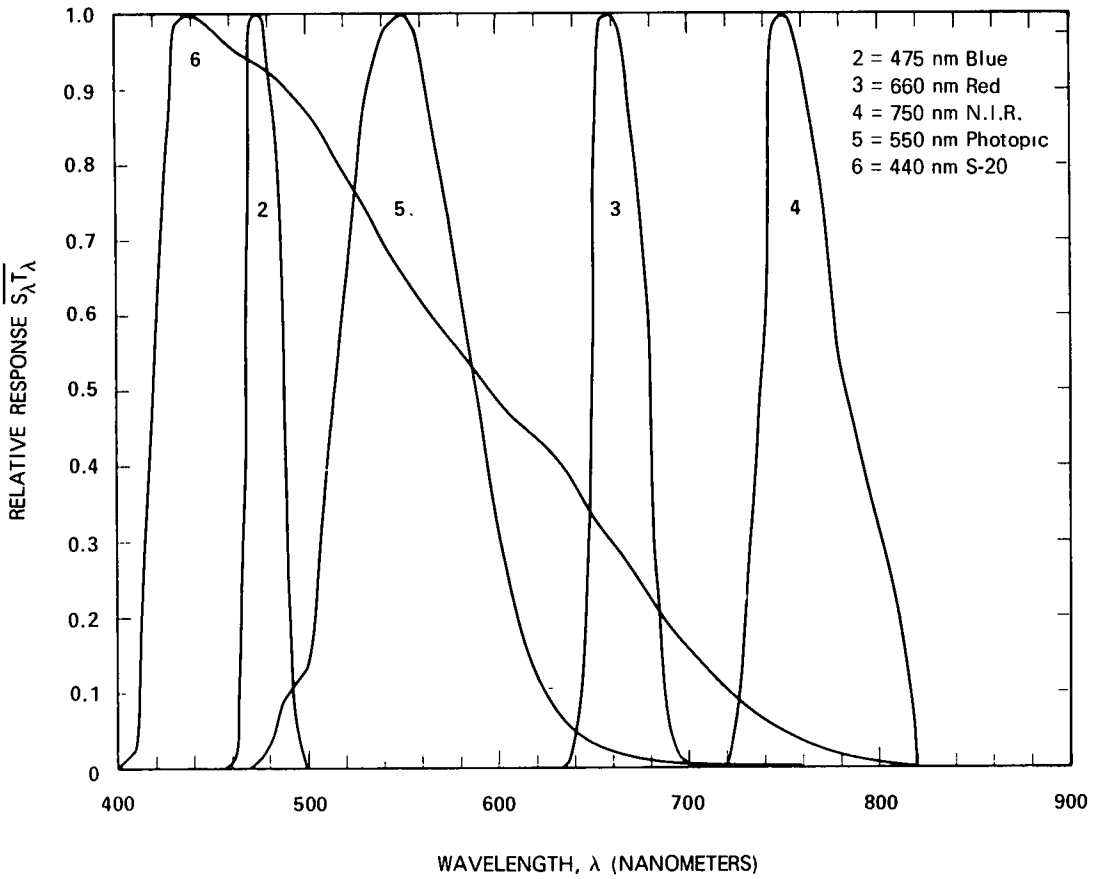

Fig. 1-1. Standard Spectral Responses.

A summary of the methods used in the derivation of the reported optical atmospheric properties is discussed in Section 2, as are the various modifications to the techniques which have been instituted during this contract interval.

The optical instrumentation, developed at the Visibility Laboratory, has been reported in detail in Duntley, *et al.* (1970) and Duntley, *et al.* (1972a and b). The portions of this instrumentation, installed in USAF C-130A SN50022, that generated the raw data upon which the reported properties are based consisted of an integrating nephelometer for determining the total scattering coefficient and two sky scanning radiometers for recording upper and lower sky radiances. A ground-based integrating nephelometer similar to the airborne instrument provided the ground-level value of the total volume scattering coefficient. Major revisions to the hardware have occurred at several intervals during the life of this current contract. They are summarized and discussed in Section 3.

Data collection methods throughout this report interval have remained similar to those described in Duntley, *et al.* (1972a and b). A short review of the technique is discussed in Section 4. A tabulation of the resulting data bank is shown in Table 1-1.

The computer techniques used during this report interval are also well-documented in the previously identified references. A summary of the most significant alterations introduced during this contract interval, as well as a summarization of the processing procedure for the existing data backlog, is presented in Section 5.

Section 6 presents a review of the field trips and a summary of the existing data bank and its status.

Section 7 reviews portions of the data previously reported during the contract interval. Additional data measured by the contrast reduction meter during the field trip to central New Mexico and selected scattering coefficient profiles measured near St. Louis, Missouri, are also included.

A discussion of projected procedural updates and recommendations for future program activities is included in the concluding section, 8.

2. THEORY

2.1 AIRBORNE DATA DERIVATIONS

The two scientific reports from this contract period, Duntley, *et al.* (1972a and b), contain the optical properties of various downward-inclined paths of sight based on daytime atmospheric optical measurements. These properties include irradiance upon horizontal plane surfaces, directional background reflectance, total volume scattering coefficient, beam transmittance, path radiance, and path reflectance.

The methods used in the derivation of these optical properties are discussed in detail in Section 2 of Duntley, *et al.* (1972a and b). There are four principal modifications from the methods outlined in Duntley, *et al.* (1970). First, extrapolations of total volume scattering coefficient are made according to the density ratios of the U. S. Standard Atmosphere (1962). Second, the refraction effect has been added to the effect of earth curvature for the computation of the incremental path length for the near horizontal slant paths. Third, the selection of the shape of the volume scattering function from the Barteneva (1960) catalog is now based upon the *in situ* measurements of the volume scattering function at 30 and 150 degrees. Finally, when the sky near the sun is unclouded, the apparent sun radiance value is based upon the theoretical value of the sun radiance out-of-the-atmosphere and the beam transmittance from out-of-the-atmosphere to the altitude of measurement (based on an extrapolation of beam transmittance from the highest flight altitude).

GENERAL APPROACH

Path radiance in the downward direction in the troposphere is not a directly measurable quantity. The current method of deriving path radiance was originally developed for the low light-level case of a starlight night. The basic method is one of computing the path function and then integrating over the path length to get path radiance. The path function $N_*(z,\theta,\phi)$ at altitude z, zenith angle θ, and azimuth ϕ is computed from measured values of sky and terrain radiance $N(z,\theta',\phi')$:

$$N_*(z,\theta,\phi) = \int_{4\pi} N(z,\theta',\phi')\,\sigma(z,\beta')\,d\Omega\,. \qquad (2.1)$$

The relative nondirectionality of the sky light during starlight de-emphasized the need for a precise evaluation of the directionality of the volume scattering function $\sigma(z,\beta)$. The β is the scattering angle between the path of sight and the sky or terrain radiance.

When this method was adapted for use during the higher and more directional light levels encountered during moonlight, careful specification of both the sky and moon radiance became imperative. Fortunately, the dynamic range of measurement for the upper hemisphere scanner was such that the moon radiance was on scale for all but one filter. Also, the precision of the sky measurements for moonlight was enhanced by slowing down the scanner rate.

Since the directionality of the volume scattering function also became more important for moonlight, the measurement of the volume scattering function at 30- and 150-degree scattering angles by the integrating nephelometer became of some importance. Difficulties with the $\sigma(\beta)$ measurements encountered during the earlier contract period reported in Duntley, *et al.* (1970) have been surmounted and valid $\sigma(\beta)$ values are available for all the daytime optical measurements.

When the scanner was adapted to daytime flux levels it was found that sun radiances were generally above the calibrated range of the instrument. This led to the modification of the computational technique which substituted a sun radiance value based upon the theoretical value for out-of-the-atmosphere and an extrapolated beam transmittance.

The path function at night, under starlight or moonlight conditions, is not directly measurable because of the low flux levels involved. It is measurable, however, during daytime, hence the addition of the variable path function meter to the daytime airborne instrumentation. Path function measurement is difficult even in daytime since it is a scattered light measurement, low in flux relative to the ambient lighting. The current instrument is still in the development stages as described in detail in Section 3.

MODIFICATIONS COMPLETED

Continued concern about adequate specification of the sky and sun radiances, and the volume scattering function has led to a number of recent modifications to measuring and computational techniques. These modifications are not contained in the two scientific reports, Duntley, *et al.* (1972a and b).

One modification, completed in January 1972, allows for the addition of a separate sun mode scanner interval to the measurement pattern. During these measurements the radiances of the sun and the sky in the immediate surround are within the calibrated range of the instrument. This modification is described in detail in Section 4.1.

A computational technique modification was completed in May 1972. The primary change was to separate the sun radiance from the scanner radiances. Thus, for the path function, Eq. (2.1) becomes

$$N_*(z,\theta,\phi) = {}_sN_r(z,\theta_s,0^\circ)\,\sigma(z,\beta) + \int_{4\pi} N(z,\theta',\phi')\,\sigma(z,\beta')\,d\Omega\,. \qquad (2.2)$$

Similar changes were made to computations of downwelling irradiance and scalar irradiance. In this way the exact sun zenith angle could be used in all computations specifying position. One result is more accurate assignment of cosine weighting for the sun component of the flat plate irradiance.

Since one of the sources of variability in the data for a given flight is the change in sun zenith angle over the flight interval, an option was added which allows the use of an average sun zenith angle in the computations of path radiance and irradiances. An option was also added to allow external specification of the space-to-highest-flight-altitude beam transmittance. This was originally designed to be used for cloudy days with an estimated beam transmittance. However, it can also be used to insert the value of beam transmittance obtained by ratioing the space-to-earth transmittance measured by the contrast reduction meter and the high-altitude-to-earth transmittance from the nephelometer data, as suggested in Section 8 of Duntley, *et al.* (1972b).

MODIFICATIONS IN PROCESS

Beam Transmittance from Sky Radiance Ratios. Another method of obtaining beam transmittance from space to highest flight altitude is being explored. This method stems from the suggested nomographic method of Kushpil'and Petrova (1971) for obtaining beam transmittance from sky radiance ratios at equivalent scattering angles from the sun. Kushpil' and Petrova do not give equations for the sky radiance ratio as a function of beam transmittance, but such an equation may be derived from relationships previously developed from our own work.

A sky radiance is a path radiance from out of the atmosphere to the altitude of measurement $N^*_\infty(z,\theta,\phi)$. On clear days with no absorption, we have found the sky radiance to be a function of an effective equilibrium radiance $\bar{N}_q$ and the beam transmittance [Gordon, *et al.* (1963), Gordon (1969), and Gordon, *et al.* (1972)]:

$$N^*_\infty(z,\theta,\phi) = \bar{N}_q(z,\theta,\phi)\,[1 - T_\infty(z,\theta)] \,. \tag{2.3}$$

Thus the ratio of two sky radiances, at angles θ and θ', would be

$$\frac{N^*_\infty(z,\theta,\phi)}{N^*_\infty(z,\theta',\phi')} = \frac{\bar{N}_q(z,\theta,\phi)}{\bar{N}_q(z,\theta',\phi')} \; \frac{[1 - T_\infty(z,\theta)]}{[1 - T_\infty(z,\theta')]} \,. \tag{2.4}$$

When the scattering angle from the sun is equivalent for the two paths of sight, the equilibrium radiances are equivalent. Thus Eq. (2.4) simplifies to

$$\frac{N^*_\infty(z,\theta,\phi)}{N^*_\infty(z,\theta',\phi')} = \frac{[1 - T_\infty(z,\theta)]}{[1 - T_\infty(z,\theta')]} \,. \tag{2.5}$$

Equation (2.5) can be expressed as a function of the vertical transmittance $T(z,0°)$ and the relative optical airmass $m_\infty(z,\theta)/m_\infty(z,0°)$:

$$\frac{N^*_\infty(z,\theta,\phi)}{N^*_\infty(z,\theta',\phi')} = \frac{\left[1 - T_\infty(z,0°)^{m_\infty(z,\theta)/m_\infty(z,0°)}\right]}{\left[1 - T_\infty(z,0°)^{m_\infty(z,\theta')/m_\infty(z,0°)}\right]} \,. \tag{2.6}$$

Equation (2.6) cannot be directly solved for the vertical transmittance, but by using iterative means, which is a simple task with a computer, a vertical transmittance can be obtained which provides a solution to Eq. (2.6) within any prescribed precision tolerance.

An error analysis of the equation indicates that the precision error difference of the two radiances is generally multiplied by a factor of between 1 and 2 for many zenith angle combinations. Thus, use of a series of measurements and averaging would enhance the reliability of the resultant transmittance.

This technique was applied to the sky radiances at the highest flight altitude for three flights made in central New Mexico, Flights C-154, C-155, and C-157. These are presented in Column 8 of Table 2-1.

Transmittances for space to ground $T_{\infty}(0,0°)$ were available from the contrast reduction meter (CRM) for these flights (Column 5) as well as beam transmittances altitude to ground $T_r(0,0°)$ based on the airborne nephelometer measurements (Column 6) [Duntley, *et al.* (1972b)]. From these two measured values a space-to-altitude beam transmittance $T_{\infty}(z,0°)$ (Column 7) was computed by

$$T_{\infty}(z,0°) = \frac{T_{\infty}(0,0°)}{T_r(0,0°)} . \qquad (2.7)$$

Table 2-1

Vertical Beam Transmittance from Space to Highest Flight Altitude
Obtained by Three Methods

Flight No.	Date 1970	Filter	Altitude (m) AGL	CRM $T_{\infty}(0,0°)$	Nephelometer $T_r(0,0°)$	CRM and Nephelometer $T_{\infty}(z,0°)$	Sky Ratio $T_{\infty}(z,0°)$	Nephelometer Extrapolation $T_{\infty}(z,0°)$
C-154	28 Oct	2	4375	0.568	0 698	0.813	0.822	0.563
↓	↓	5	4375	0.623	0.769	0.810	0.875	0.655
↓	↓	3	4375	0.673	0.809	0.832	0.913	0.709
C-155	30 Oct	2	4350	0.571	0.703	0.812	0.813	0.556
↓	↓	5	4327	0.637	0.764	0.833	0.870	0.613
↓	↓	3	4331	0.680	0.812	0.837	0.880	0.670
C-157	3 Nov	2	4374	0.526	0.711	0.740	0.829	0.672
↓	↓	5	4358	0.592	0.788	0.751	0.704	0.779
↓	↓	3	4367	0.637	0.829	0.768	0.777	0.823

These values in Column 7 comprise the most direct means available of measuring $T_{\infty}(z,0°)$.

The final column, 9, contains the values of transmittance obtained by using the nephelometer measurement at altitude z of the total scattering coefficient s(z) and the scale height at altitude H(z) [Eq. (2.27) in Duntley, *et al.* (1972a and b)]:

$$T_{\infty}(z,0^{\circ}) = e^{-H(z)s(z)}. \tag{2.8}$$

This latter is the method used in Duntley, *et al.* (1972a and b) for extrapolating the beam transmittance used in computing the apparent sun radiance.

The sky radiance ratio method Eq. (2.6) and the nephelometer extrapolation method Eq. (2.8) are graphed as a function of the measured transmittance Eq. (2.7) in Fig. 2-1. The sky radiance ratio method is a decided improvement over the extrapolation method for two of the flights, C-154 and C-155, and roughly comparable for Flight C-157.

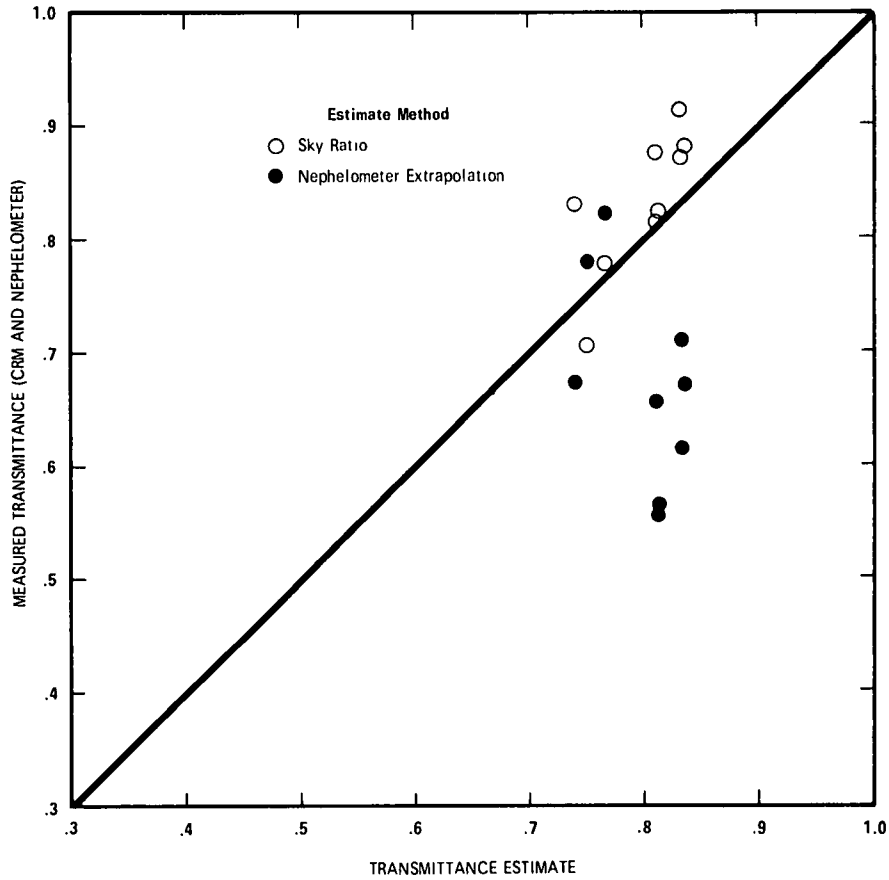

Fig. 2-1. Comparison of Methods for Obtaining Vertical Beam Transmittance Space to Highest Altitude of Flight $T_{\infty}(z,0)$ for Flights C-154, C-155 and C-157.

The values in Column 8 were obtained using a zenith angle for each radiance based on the assumption that the scanner angular pattern was a true spiral and consistent in rate of angular changes. Recent inspection of the angular position as measured during flight indicates sufficient difference from the theoretical pattern to warrant use of the measured angular positions for applications such as in Eq. (2.6), where angular error contributes substantially to the final error in transmittance. The next step in developing the sky radiance ratio method will be re-evaluation of Eq. (2.6) using measured zenith angles for the radiances to see if the resultant transmittances are correspondingly increased in accuracy.

Proportional Directional Scattering Function. An attempt is also currently in progress to recover the proportional directional scattering function $\sigma(z,\beta)/s(z)$ from the sky radiances. The equation being used is Eq. (23) from Gordon (1969):

$$\sigma(z,\beta)/s(z) = \left[\bar{N}_q(z,\theta,\phi) - \frac{{}_kh(z,d) + h(z,u)}{4\pi} \right] \div \left[{}_sh(\infty)\, T_\infty(z,\theta_s) \right], \qquad (2.9)$$

where ${}_kh(z,d)$ is the scalar irradiance from the sky, $h(z,u)$ is the upwelling scalar irradiance, and ${}_sh(\infty)$ is the inherent sun irradiance. Successful use of Eq. (2.9) depends upon an accurate $T_\infty(z,0)$ value as well as accurate sky radiances and sky position information. This recovery process is in the early stage of development.

2.2 GROUND-BASED DATA DERIVATIONS

The first scientific report, Duntley, *et al.* (1972a), contained no change from the ground-based measurement approach or data-use outlined in Duntley, *et al.* (1970). Basically, ground-based nephelometer data and terrain reflectance data were considered of primary importance although terrain reflectance data were not recovered due to data logger difficulties and data retrieval problems.

The second scientific report, Duntley, *et al.* (1972b), contained in Section 3.1 a full description of the contrast reduction meter and the methods used to derive vertical earth-to-space beam transmittance, path radiance, and path reflectance. The addition of the contrast reduction meter to the ground-based system is an important supplement to the overall (airborne and ground) system of measurements, providing an indispensable diagnostic tool [see Section 8.2, Duntley, *et al.* (1972b)].

The derivation and validation of the basic method of measuring earth-to-space path radiance from ground stations is contained in an article begun previous to but completed and submitted during this contract interval: Gordon, *et al.* (1972). Several in-house technical notes deal with the method (Technical Note 3) and the catalog of data available (Technical Notes 4 and 5) from measurements made previous to this contract period. These earlier measurements have proven useful in evaluating the current CRM measurements (see Fig. 7-2 and 7-3).

3. INSTRUMENTATION

The scientific instrumentation utilized during the interval 1 November 1969 through 31 August 1972 was first described in AFCRL-70-0137, Duntley, *et al.* (1970). In that report, the descriptions of the radiometric systems reflected the nighttime, low flux configuration for which they were initially designed and fabricated. Subsequent to that report, two additional reports were issued which review selected modifications to the basic system. The first was AFCRL-72-0255, Duntley, *et al.* (1972a) and the second, AFCRL-72-0461, Duntley, *et al.* (1972b). These two reports describe in general the basic system modifications which were required to convert the radiometric devices from nighttime to daytime operating configurations.

The atmospheric visibility program at the Visibility Laboratory is planned and organized as an ongoing program, and thus a variety of instrumentation modifications were implemented subsequent to the period reported in Duntley, *et al.* (1972b). The following paragraphs summarize the characteristics of the most significant of these recent improvements.

For the convenience of the reader, all significant instrument systems utilized during this report interval are tabulated in Table 3-1 and illustrated in their deployment configurations in Fig. 3-1 and 3-2.

Table 3-1. Project Instrumentation

I. Radiometric

- A. Multiplier Phototube Assembly
- B. Temperature Control Housing Assembly
- C. Optical Filter Assembly
- D. Radiometer Measuring Circuit Assembly
- E. Optical Collector Assembly

1. Automatic 2π Scanner Assembly
2. Integrating Nephelometer Mode Selector Head Subassembly
3. Dual Irradiometer Assembly
4. Large Aperture Telescope Assembly
5. Variable Path Function Meter Assembly
6. Equilibrium Radiance Telephotometer
7. Contrast Reduction Meter

II. Meteorological

A. Royco Model 220 Particle Counter
B. Cambridge Model 137-C3 Aircraft Hygrometer System
C. AN/AMQ-17 Aerograph Set
D. Bourns Model 430/530 Absolute Pressure Transducer
E. Bourns Model 509 Differential Pressure Transducer
F. Bendix Model 566 Aspirated Hygrometer
G. Science Associates Windspeed and Direction Set
H. Taylor Model SMT-5-51 Aneroid Barometer

III. Control and Communication

A. Automatic 2π Scanner Control Console
B. Photometer Temperature Control Panel
C. Optical Filter Control Panel
D. Ten Slide Photometer Module
E. Camera Control Panel
F. Flight Dynamics Display Panel
G. 42 Channel Data Logger
H. 20 Channel Data Logger

IV. Photographic

A. Automax G-1 Airborne Camera System
B. Ground-Based Soligor System

3.1 RADIOMETRIC SYSTEMS

MULTIPLIER PHOTOTUBE AND TEMPERATURE CONTROL HOUSING ASSEMBLIES

The multiplier phototube assembly and the temperature control housing assembly have performed reliably during the past 3 years, and no basic design changes have been instituted. The basic sensitivity of each radiometer system is established by the load resistor shown at the input to the buffer amplifier in Fig. 3-3. Two basic sensitivities have historically been associated with these radiometers. A high sensitivity mode, for use at nighttime flux levels, requires a 1000-megohm load, whereas the low sensitivity mode, used for daytime measurements, is optimized using a 10-megohm load. In early 1972, the detector assemblies assigned to the 2π automatic scanner systems were converted from high to low sensitivity. This conversion was implemented as part of a basic procedural update which is discussed more thoroughly in Section 4.

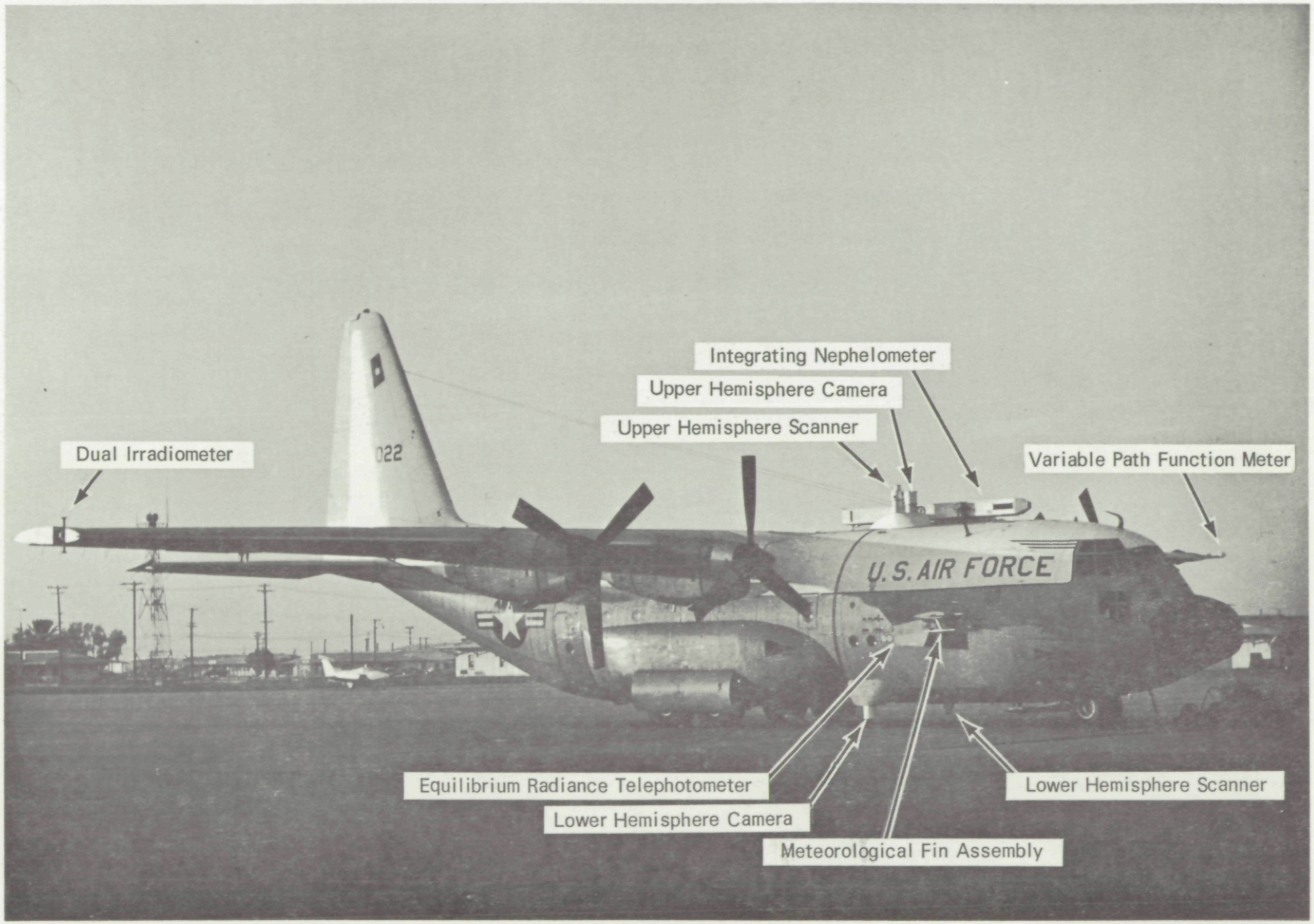

Fig. 3-1. C-130 Airborne Instrument System.

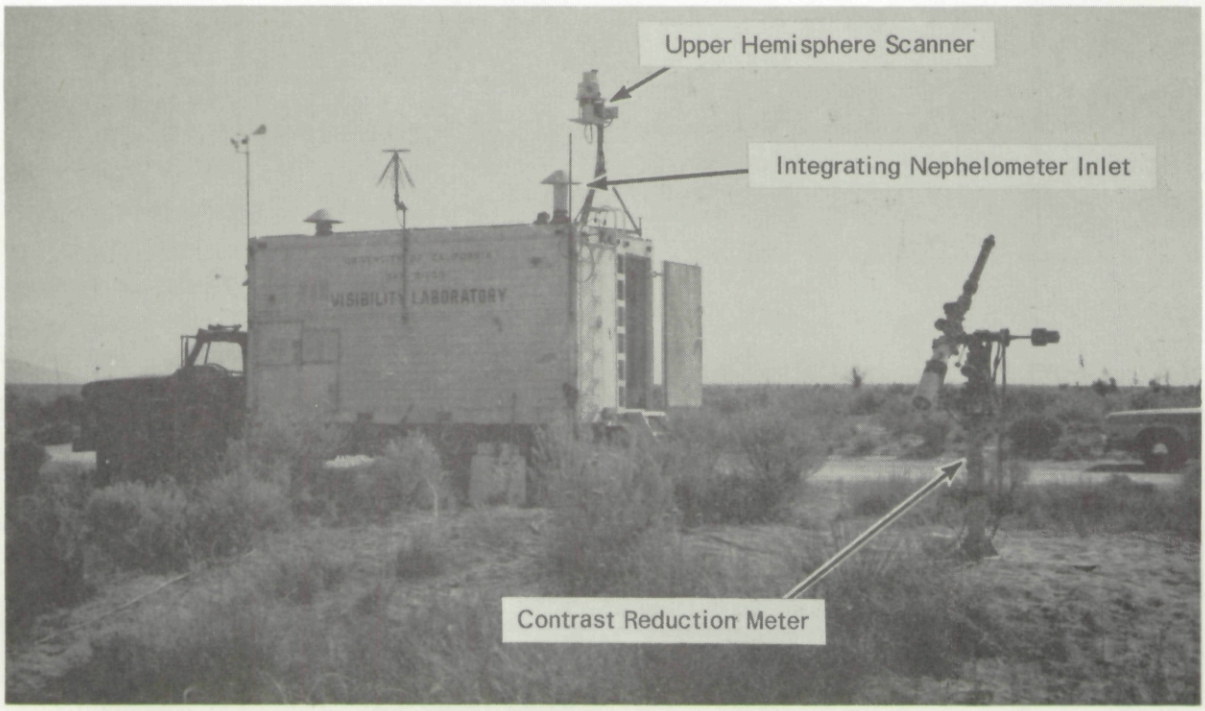

Fig. 3-2. Ground-Based Instrument System.

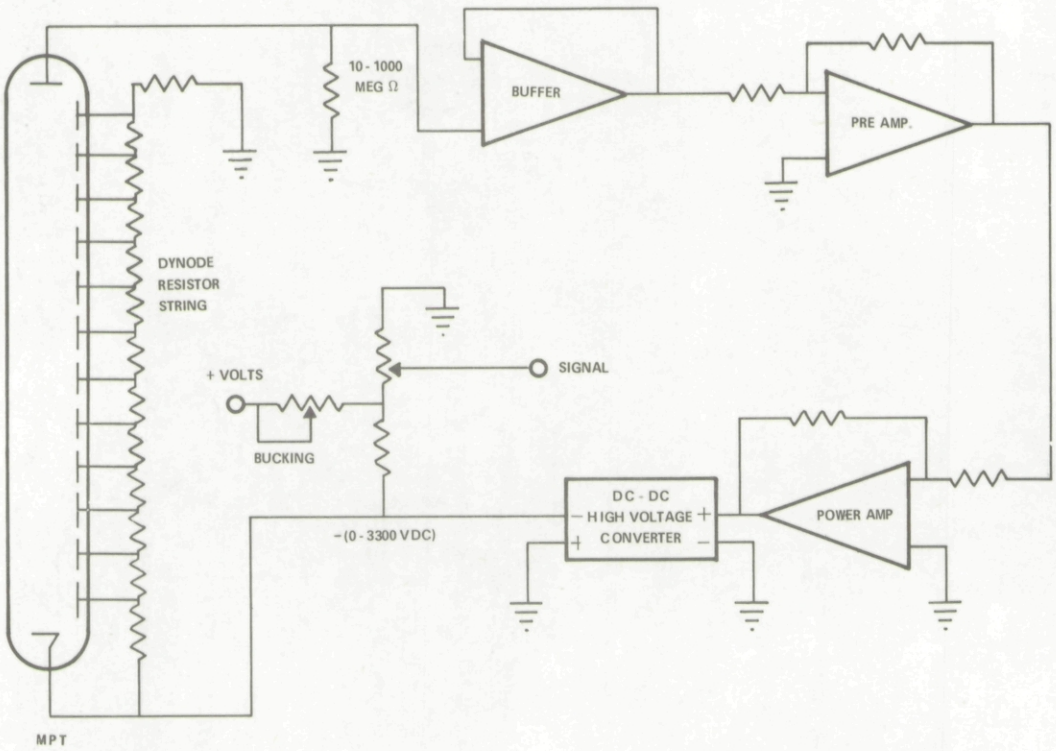

Fig. 3-3. Typical Visibility Laboratory Model 5 Photometer Circuit.

OPTICAL FILTER ASSEMBLY

The optical filter assembly has undergone a major revision since the configuration reported in Duntley, *et al.* (1972b). This device was originally designed for operation at nighttime flux levels. During the last half of calendar year 1969 it was modified to enable the simultaneous stacking of two optical filters in series along the optical path. One of these filters was designated to be of neutral density. The insertion of this neutral density filter in series with each of the original color selection filters shifted the flux level reaching the detector assembly by approximately 6 decades. This preliminary modification allowed the daytime radiance measurements reported by Duntley, *et al.* (2972a and b). Subsequent to the activities conducted under Projects HAVEN VIEW and ATOM, it became apparent that the operation of the optical filter assembly was not completely satisfactory. Consequently, between November 1970 and March 1971, a further revision of the basic device was accomplished.

The final modification to the optical filter assembly was designed to eliminate two particularly troublesome features. The first was an undesirable burst of stray light which entered the detector assembly every time the MEMORY position was selected, and the second was an ambiguous verification signal which was returned to the control panel and data logger.

The stray light problem was approached by installing an independently controlled sliding filter subassembly at the entrance port of the optical filter assembly. With this device installed, the day/night neutral density filter was electrically maintained in the optical path regardless of whether or not any other color filter or memory mirror solenoids were actuated. This alteration to the stacking sequence eliminated the undesired stray light bursts.

The ambiguous verification signal was eliminated by installing voltage divider networks in each optical filter assembly and individual monitoring voltmeters in the filter control panel. Thus, when a particular filter was selected by the operator, the feedback signal not only indicated to him that a filter had been inserted, but, via the voltage divider, also identified specifically which filter it was.

RADIOMETER MEASURING CIRCUIT ASSEMBLY

No modifications were made to the radiometer measuring circuit assemblies during this contract interval.

OPTICAL COLLECTOR ASSEMBLY

Two of the seven optical collector assemblies listed in Table 3-1 have had major modifications made to them during the period covered by this report. They are the integrating nephelometer and the variable path function meter. The most significant features of these modifications are discussed in the following paragraphs.

Integrating Nephelometer Mode Selector Head Subassembly. The integrating nephelometer was originally designed as a device for making airborne measurements at night. This configuration was described by Duntley, *et al.* (1970). The airborne shroud was initially modified to permit daytime operation prior to the HAVEN VIEW deployment as reported by Duntley, *et al.* (1972a). Only minor revisions to the

shroud have been made since this 1972 report, and they involved the addition of some interior light baffles to reduce undesirable stray light effects. A further revision to this shroud is currently in the design stage. The implementation of the design update will further reduce undesirable stray light and improve the aerosol flow characteristics through the measuring volume.

In addition to the shroud modifications, the mode selector head subassembly was completely redesigned during 1971. By January 1972, three new subassemblies had been built, tested, and put into operation. The modifications to this subassembly were designed to improve operational reliability, which was becoming poorer and poorer with each subsequent field deployment, to improve serviceability, and to improve the reproducibility of the system's internal optical alignment. The basic procedure was to replace the original prism support and solenoid stepper drive with a new support and a Geneva controlled constant drive motor. Flight programs subsequent to this modification have had excellent results from this system, with zero malfunctions.

Variable Path Function Meter Assembly. The variable path function meter assembly was discussed briefly in both AFCRL-70-0137, Duntley, *et al.* (1970) and AFCRL-72-0255, Duntley, *et al.* (1972a). There was a minor nomenclature change during the interval between the issuance of these two reports which should be noted. In the 1970 report the device was identified as the **vertical** path function meter in both the text and illustrations. However, in the 1972 report the same device was identified as the **variable** path function meter. The redesignation was made solely in the interest of descriptive accuracy and implies no material change in operational characteristics.

During early 1971 a series of data flights were made over Green Bay, Wisconsin. These flights provided experimental data which were to verify a suspected design error in the variable path function meter (VPFM) shroud assembly. Subsequent to the analysis of these data as well as selected data from the HAVEN VIEW and ATOM deployments, a major revision to the VPFM system was initiated.

Three modifications to the VPFM system have been accomplished during this report interval. Two of the three affected the optical design, while the third was a mechanical change. The instrument in its revised configuration is illustrated in Fig. 3-4.

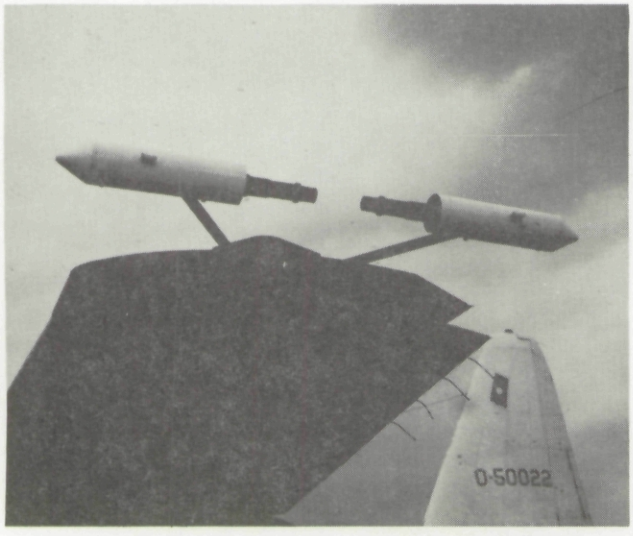

Fig. 3-4. Variable Path Function Meter.

The two optical modifications were devised to improve both stray light rejection characteristics and definition of the aerosol sampling volume. The first step was to remove the conical sunshades illustrated in AFCRL-70-0137 and to replace them with the cylindrical type shown in Fig. 3-4 of this report. This step's primary effect was to reduce the probe error generated by the conical surface's close proximity to the sampling volume. The second step was to install a new telescope assembly which increased the distance between the objective lens and the sample volume. This modification's primary result was a marked improvement in stray light rejection. The results of these optical modifications are clearly evident in the preliminary data evaluations currently being conducted upon the Laboratory's data backlog.

The mechanical modification was accomplished in order to speed up the ground time required for equipment mounting and demounting. It basically splits the variable path function meter assembly into two parts, the wingtip and the yoke. Prior to modification, the entire wingtip and the permanently attached VPFM assembly had to be removed and replaced before and after each field deployment. It was a difficult and high risk operation. Subsequent to the modification, the wingtip remained attached to the aircraft and only the protruding yoke assembly was removed. This simplification has resulted in substantially reduced turnaround times. The attendant reduction in hazard to the aircraft, the instrument system, and the crew has been an enjoyable bonus.

3.2 METEOROLOGICAL SYSTEMS

Only two modifications to the meteorological systems have been instituted during this contract interval. Both were initiated rather late in the contract period and are still in the process of completion.

ROYCO MODEL 220 PARTICLE COUNTER

The first modification request was submitted as a proposal to reroute the inlet plumbing to the Royco particle counter. The original inlet plumbing for this system was partially illustrated in AFCRL-70-0137, Duntley, *et al.* (1970), Fig. 3-15 and 3-16. The utilization of this original plumbing required the sample aerosol to traverse a long and tortuous path between the inlet probe and the sampling chamber. There was no provision for cleaning and purging the inlet tubing. Both of these features contributed to a severe compromise of the confidence levels associated with the system's output. A new plumbing installation is currently being accomplished to overcome the basic deficiencies of the original design. The modification is scheduled for use beginning in November 1972.

CAMBRIDGE MODEL 137-C3 AIRCRAFT HYGROMETER SYSTEM

The second modification to the meteorological systems is related to the Cambridge hygrometer. This system is illustrated in AFCRL-70-0137, Duntley, *et al.* (1970), Fig. 3-17 and 3-18. During the analysis of the flight data from Projects HAVEN VIEW and ATOM, severe anomalies were found in the dewpoint temperature profiles. After considerable investigation and testing, it became apparent that a system update was required. Consequently, in early 1972 two new subassemblies, a model 912C control amplifier and a model 137A-20 mounting fixture, were acquired. The installation of these new subassemblies will be completed prior to the resumption of the aircraft flight schedule. The new sensor mounting fixture is illustrated in Fig. 3-5.

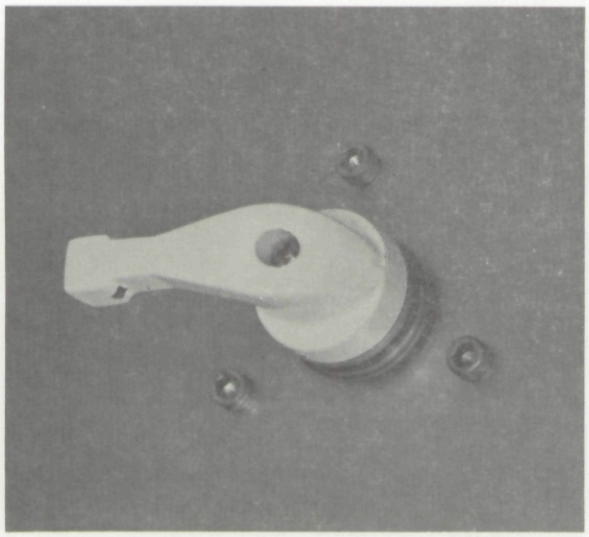

Fig. 3-5. Cambridge Model 137A-20 Probe Housing.

3.3 CONTROL AND COMMUNICATION SYSTEMS

The control panels, consoles, and other support facilities listed in Table 3-1 are described in their original configuration by Duntley, *et al.* (1970). Only two of the eight items listed have had major modifications, the 2π scanner control console and the optical filter control panel. Additionally, the 42 channel data logger has been updated to provide parallel monitoring. The pertinent alterations are discussed briefly in the following paragraphs.

AUTOMATIC 2π SCANNER CONTROL CONSOLE

Of the six individual control panels that constitute the control console, only one has been modified. The "programmer panel" contains the solid state logic which controls the actual automatic pattern that the scanner field of view traverses.

The original pattern called for a full 2π steradian search, plus reset, in 32 seconds. The azimuth drive was constant at one revolution per second. The elevation drive followed a variable rate ramp function. This scan rate was too fast for many applications and consequently a timing modification was inserted to slow the entire routine down to one fifth its original speed. In this slower mode the full 2π steradian search was accomplished in 160 seconds, with the azimuth sweep constant at 5 seconds per revolution. The 160-second pattern was used throughout the Project HAVEN VIEW and ATOM deployments.

With the advent of several data processing sophistications, it became apparent that further scan pattern alterations were necessary. Consequently, in early 1972 a major revision to both the airborne and ground-based programmer panels was instituted. The salient features of this modification effort were as follows:

A. In contrast with the scheme originally established, as in Duntley, *et al.* (1970), both airborne and ground-based programmers were converted to generate the same search pattern.

B. The primary azimuth drives were slowed to 10 seconds per revolution. On the airborne system, the rate selector switch was altered to allow the operator to select azimuth rates of either 1, 5, or 10 seconds per revolution, at his discretion.

C. The elevation drives were changed to yield a constant step of 5 degrees in elevation at the completion of each azimuth sweep. In the automatic mode, the elevation angle for the first revolution was set at 2-1/2 degrees to reduce horizontal clutter induced in the 5-degree field of view.

The resultant sweep pattern now utilized by all automatic 2π scanners is illustrated in Table 3-2.

Table 3-2

Automatic 2π Scanner Sweep Pattern

Azimuth Revolution No.	Constant Elevation Angle	Upper Hemisphere Zenith Angle	Lower Hemisphere Zenith Angle
1	2.5°	87.5°	92.5°
2	7.5°	82.5°	97.5°
3	12.5°	77.5°	102.5°
4	17.5°	72.5°	107.5°
5	22.5°	67.5°	112.5°
6	27.5°	62.5°	117.5°
7	32.5°	57.5°	122.5°
8	37.5°	52.5°	127.5°
9	42.5°	47.5°	132.5°
10	47.5°	42.5°	137.5°
11	52.5°	37.5°	142.5°
12	57.5°	32.5°	147.5°
13	62.5°	27.5°	152.5°
14	67.5°	22.5°	157.5°
15	72.5°	17.5°	162.5°
16	77.5°	12.5°	167.5°
17	82.5°	7.5°	172.5°
18	87.5°	2.5°	177.5°
	Airborne direct reset		
19	Ground system reset during revolution 19 and 20		
20	Ground system reset during revolution 19 and 20		

This new scan pattern has been utilized on all data missions conducted subsequent to 15 January 1972. The preliminary data dumps indicate a marked improvement in orientation stability and good response to operator-induced changes in revolution speed.

OPTICAL FILTER CONTROL PANEL

Several minor rewiring modifications have been made on the optical filter control panel. These rewires were in general devised to accommodate the simultaneous filter stacking discussed in Section 3.1. The only mechanical modification to the panel during 1971 was the insertion of individual voltmeters in lieu of the originally provided indicator lamps. Subsequent to several data missions using this new configuration, it became apparent to the data analysis team that the voltmeter verification technique was too powerful a diagnostic tool not to be recorded on tape. As a result of this enlightenment, a major panel revision was initiated in early 1972, the result of which is illustrated in Fig. 3-6.

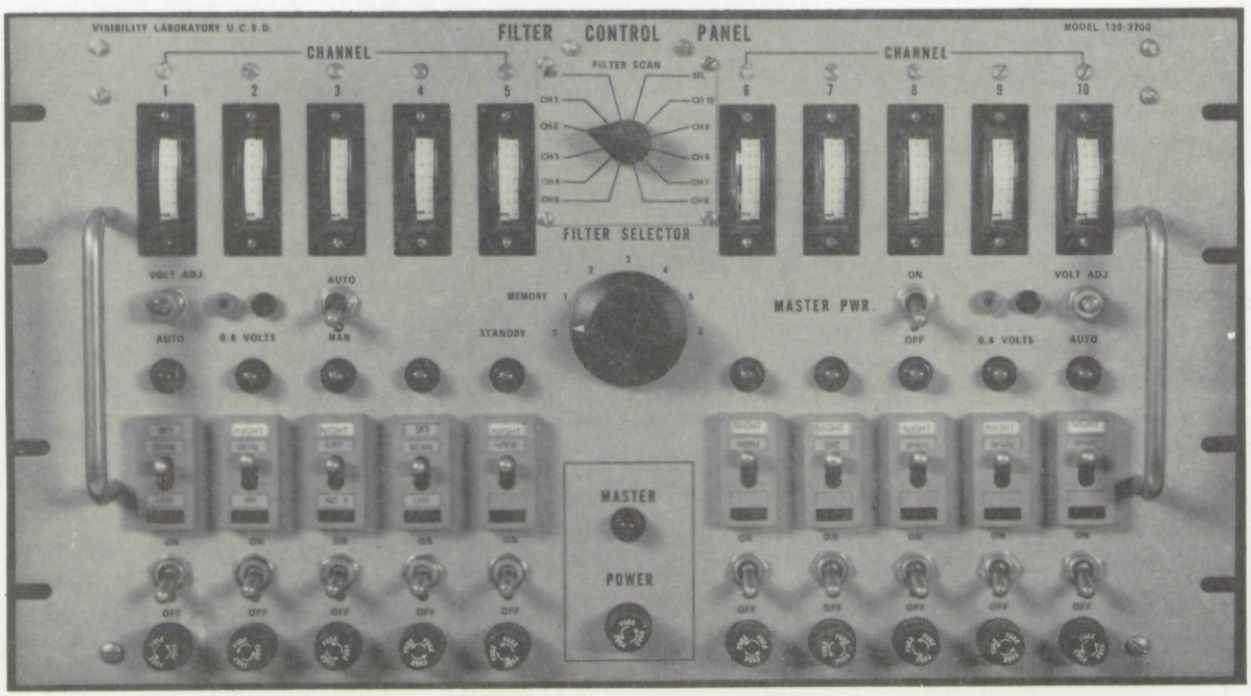

Fig. 3-6. Optical Filter Control Panel

The current model of the optical filter control panel was built to provide procedural simplifications for the operator, as well as provide additional information to the data logger. First, the control circuitry was reduced from 14 independent channels to only 10. This reduction in number has allowed the institution of a symmetric panel layout which materially reduces operator error during flight. Second, the day/night filter control was completely isolated from the spectral filter control. This change in wiring logic protects the multiplier phototube from the spurious bursts of high flux levels discussed in Section 3.1. The third major item in the panel revision was the addition of an intervalometer-driven multiplexer

which provides filter identification data from each radiometer system to the data logger. This feature provides recorded data adequate for detecting both equipment and /or operator malfunction through automatic data processing techniques.

42 CHANNEL DATA LOGGER

The 42 channel data logger is discussed in both previously referenced reports, AFCRL-70-0137 and AFCRL-72-0255. One basic shortcoming of the recording system was the operator's inability to simultaneously monitor the logger's input channels while the data were being recorded on tape. This lack of real-time monitoring capability severely compromised in-flight troubleshooting techniques. It also made the manual recording of backup data inconvenient and unreliable. In order to overcome these faults, a parallel input circuit was devised which included channel selector switches, channel identification nixies, and an independent digital readout. The addition of this parallel monitoring subassembly has greatly enhanced the reliability of the field data and contributed significantly to the increased flexibility of the logger's in-house utilization.

3.4 PHOTOGRAPHIC SYSTEMS

No major modification to either the airborne or ground-based photographic systems has been made since the installation was reported in AFCRL-72-0461, Duntley, *et al.* (1972b). Two minor updates, however, have been accomplished to improve overall Automax G-1 system efficiency. First, new custom-built film spools were designed and fabricated at the Visibility Laboratory to improve the bearing surface at the drive spindle. This improvement should prevent the reoccurrence of a severe wear problem which contaminated the film magazine with aluminum dust. Second, orientation pegs were added to the camera housing to aid the photo-interpreter in establishing the directional orientation of the lower hemisphere photographs.

4. DATA COLLECTION METHODS

During this contract interval, two independent data-gathering activities were maintained simultaneously. The airborne instrument system was one activity and the ground-based instrument system was the other. The basic concept of each experiment was built around the joint operation of these two systems in a highly coordinated and simultaneous measurement routine. The procedural routine during each deployment was for each system to run full data collection sequences at every opportunity, on a daily schedule. If for any reason the joint sequences were aborted, both systems were to automatically revert to independent operation. Partial data sets were thus often obtained even when the inevitable exigencies of joint field operations defeated the basic routine. The general procedures followed by the airborne and ground-based teams are well-documented in Duntley, *et al.* (1970) and Duntley, *et al.* (1972a and b). Only a few comments regarding specific variations in the procedural priorities seem appropriate at this time, and they are contained in the following paragraphs.

4.1 AIRBORNE SYSTEM

The airborne data collection was accomplished through the use of an instrumented C-130A aircraft in a manner similar to that reported in AFCRL-70-0137, Duntley, *et al.* (1970) and AFCRL-72-0255, Duntley, *et al.* (1972a). During each data collection flight, the aircraft flew a predetermined pattern within the specified test area. An illustration of a typical flight pattern is shown in Fig. 4-1. In this stylized pattern, two basic elements, the straight and level and the vertical profile, are combined to yield the total mission flight plan. A more detailed description of all flight pattern elements is presented in the above referenced reports. However, in general, the data collection sequence for the airborne system has historically been broken into five standardized elements: (1) preflight warmup and calibration check, (2) straight and level sequences, (3) vertical profile sequences, (4) in-flight calibration checks, and (5) postflight calibration check. During any specific deployment, the flight profile is customized by making minor variations in the accomplishment of these five elements.

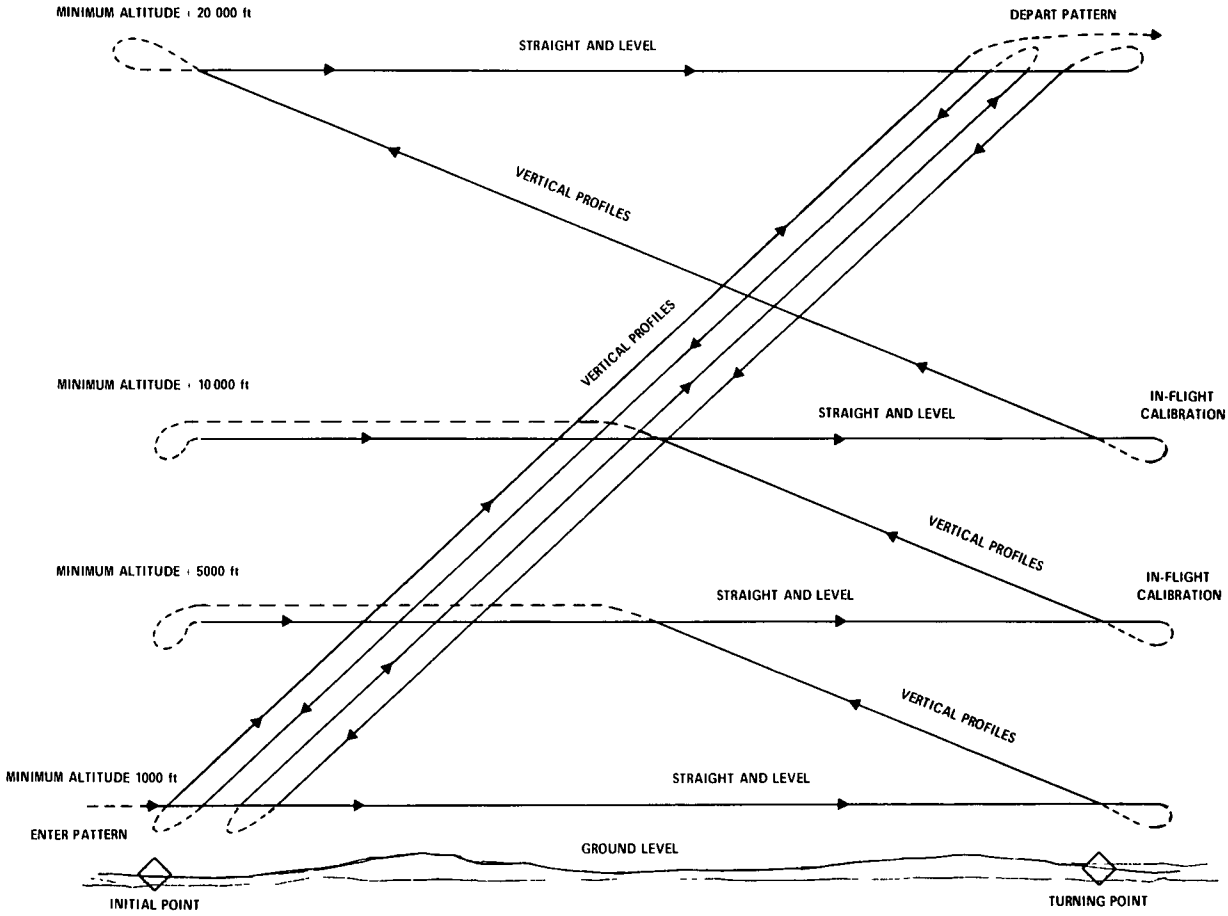

Fig. 4-1. Typical Atmospheric Visibility Program Flight Profile.

The most common variation to the flight pattern shown on Fig. 4-1 is an alteration in the altitude increments. The vertical separation between the straight and level runs is often altered to accommodate changes in local weather conditions and/or special requirements dictated by the specific problem application for which the data are being gathered. As an example, for the data reported in AFCRL-70-0137, the flight pattern was flown at night with five straight and level passes made between the ground and 1500 meters (5000 feet) above the ground; however, for the data reported in AFCRL-72-0255, the flight pattern was adjusted to be flown in the daytime with four straight and level passes made between the ground and 6100 meters (20 000 feet) above the ground.

CROSS-CALIBRATION MODE

In-flight cross-calibration procedures have been markedly improved during this contract interval. Initially, calibration stabilities were monitored only by intermittent measurements of each radiometer's self-contained Isolite reference source. However, subsequent to the deployments reported by Duntley,

et al. (1972a and b), it was decided that an additional field control was necessary to interrelate the measurements made by the upper hemisphere scanner (UHS) and the lower hemisphere scanner (LHS). As a result of this need, an additional flight element was added to the in-flight calibration check list. This element was specified as the cross-calibration (XCAL) routine.

The cross-calibration routine is inserted into the flight pattern immediately preceding the first straight and level element and is repeated immediately following the last straight and level element. During the XCAL maneuver, the automatic 2π scanners (UHS and LHS) are manually directed to look dead ahead and parallel with the aircraft flight axis. The equilibrium radiance telephotometer (ERT) is also switched to manual control and set into the same forward look as the scanners. The aircraft is put into a nose-high climb attitude and maintains this condition for 2-1/2 minutes. During this climb, the three forward-looking telephotometers (UHS, LHS, and ERT) simultaneously measure the radiance of the same piece of sky directly ahead of the aircraft. By aiming the aircraft at a reasonably uniform portion of the sky, in a direction away from the sun, one obtains a data set representing the simultaneous measurement of a common scene by three different radiometer systems. These data are automatically processed to validate and, if necessary, update the system calibration constants prior to final data processing. The cross-calibration procedure was inserted as a standard flight element, to be included on all data flights, beginning with Flight C-180, 11 August 1971.

SUN/SKY MODE

A general discussion of the theoretical basis for the computation of many optical atmospheric properties is contained in Section 2 of Duntley, *et al.* (1972a and b) and is further commented upon in Section 2 of this report. As one will note from the references, a very basic input to the computation of most of these properties is an accurate and complete data array representing the radiance distribution of the entire sky. This array must be particularly reliable in the vicinity of the sun and its aureole, since the exceptionally high radiances in these regions are the major contributors to the directionality of the overall light field.

During the early stages of this contract interval, the automatic 2π scanners were unable to fully cope with the operational demands imposed by the radiance gradients near the sun. The day/night conversion described briefly in Duntley, *et al.* (1972a) and Section 3 of this report was inadequate to accommodate the measurement of these severe radiance gradients. Consequently, a computed value for apparent solar radiance was generated and inserted into the sky radiance data array. While this technique was conceptually sound, it possessed severe real-world limitations. In order to circumvent these limitations, two system variations were accomplished.

First, the radiometric sensitivity of the 2π scanner system was electrically reduced to permit operation at normally encountered daylight flux levels. Second, the neutral density filter assigned to the system was adjusted to shift the input flux by only three decades. The double adjustment of the system's sensitivity resulted in two new operating levels. The first was designated "hard daylight," which indicated a sensitivity adjusted to measure typical sky radiances (except for the solar regions) without the insertion of the neutral density filter. The second was designated "sun mode," which indicated a sensitivity adjusted to measure typical sun and aureole radiances whenever the neutral density filter was inserted into the optical path.

The sun/sky modification described in the preceding paragraph was completed in early January 1972. To take advantage of the newly devised capability, the operational sequence during the straight and level flight sequences was also modified. This procedural modification added a series of measurements in the "sun mode" to each existing sequence of "sky mode" measurements. Thus, two data arrays were generated covering the upper hemisphere, one containing data on the entire sky except for the sun and its surround and the other containing data only on the sun and its surround. From these two arrays, a single composite array containing valid data points for the entire upper hemisphere is easily derived.

The capability for generating this composite array was included on all data flights subsequent to C-193, 25 January 1972.

A brief summary of the data flights made during this contract interval and using the general procedures discussed in Section 4.1 is presented in Table 1-1. It should be recalled that the project titles used in Table 1-1 are for identification only and are not necessarily utilized or recognized by agencies or organizations outside the Visibility Laboratory. A more complete review of the data flights is presented in Section 6.

4.2 GROUND-BASED SYSTEM

The ground-based data collection sequence was designed to supplement the airborne data whenever the aircraft was operating in the immediate vicinity. However, it is also complete enough to stand alone when the aircraft mission is diverted or aborted. The general operating procedures have been described in the references noted in Section 4.1.

The ground-based instrument system has several operational responsibilities. First, it must supply a ground-level data base to allow interpolation of various measurements between ground altitude and the lowest attainable aircraft altitude. Second, it must supply long term temporal sampling of those meteorological and radiometric quantities which relate to the project task. Third, the ground system serves as a spare parts and repair facility for the entire air/ground operation. In the event of a catastrophic failure in a primary airborne instrument or assembly, the equivalent piece of instrumentation is reassigned to the aircraft from the ground-based system. The aircraft can then return to service with a minimum of "downtime" and repairs can be accomplished under the more convenient ground station conditions.

The variations in ground-based procedures which have been instituted during this contract interval are primarily due to the addition of the contrast reduction meter (CRM), Duntley, *et al.* (1972b), to the instrument package and the resultant alteration of basic data collection priorities.

Prior to the permanent inclusion of the CRM in the instrument package, the ground-based sequence had as its primary responsibility the measurement of ground-level scattering coefficient and inherent terrain reflectance, in that order. These data were utilized for end points on the altitude to ground scattering coefficient profiles and were used in the computation of typical ground to altitude contrast transmittances.

However, during the evaluation of the Project ATOM data, it became apparent that the use of earth-to-space beam transmittances, as determined with the CRM system, was among our most valuable tools in

determining the space-to-altitude beam transmittances needed for evaluating high altitude apparent solar radiances. Recognition of this fact by the data analysis team led to a basic revision of the ground-based data collection priorities. At the present time, ground-based operating procedures have been altered to assure that measurements of earth-to-space beam transmittance in the immediate vicinity of the flight track are the activity having top priority. Backing up this activity, and still of significant importance, are the measurements of ground-level scattering coefficient and inherent terrain reflectance.

5. DATA PROCESSING TECHNIQUE

As in any reasonably complex, multi-input sampled data system, there is a large amount of data-handling required before the scientific analyst ever sees the package. The degree of data processing sophistication utilized during this contract interval is illustrated in Fig. 5-1. In this generalized flow chart, the step-by-step data processing of the raw field data is illustrated in a manner convenient for project organization and control, and does not therefore illustrate all available subroutines. A more complete description of each phase of the processing sequence is contained in Duntley, *et al.* (1972a).

During the contract interval covered by this report, the major software effort was to smooth out and efficiently implement the procedures illustrated in Fig. 5-1. Faced with the familiar problem of increasing data backlog and interpretive demands without a comparable increase in available budget, it became imperative that perturbances to the software flow be eliminated. The procedural approach was to treat each data flight as an independent data item and to process it in a heavily stylized and routine manner. As a result of this approach, the data analyst has been able to relegate a large portion of the data diagnostic tests to automatic or semi-automatic techniques, thus freeing himself for more creative interpretive efforts. The iterative nature of this routine processing has the further advantage of rapidly demonstrating inefficiencies in the technique. Since each set of flight data is handled identically, the elimination of any programming inefficiency automatically updates the quality of all subsequent sets. Since the data backlog is growing, there is continuing incentive to implement programming updates which yield outputs that are more rapidly and directly usable by the scientific analyst.

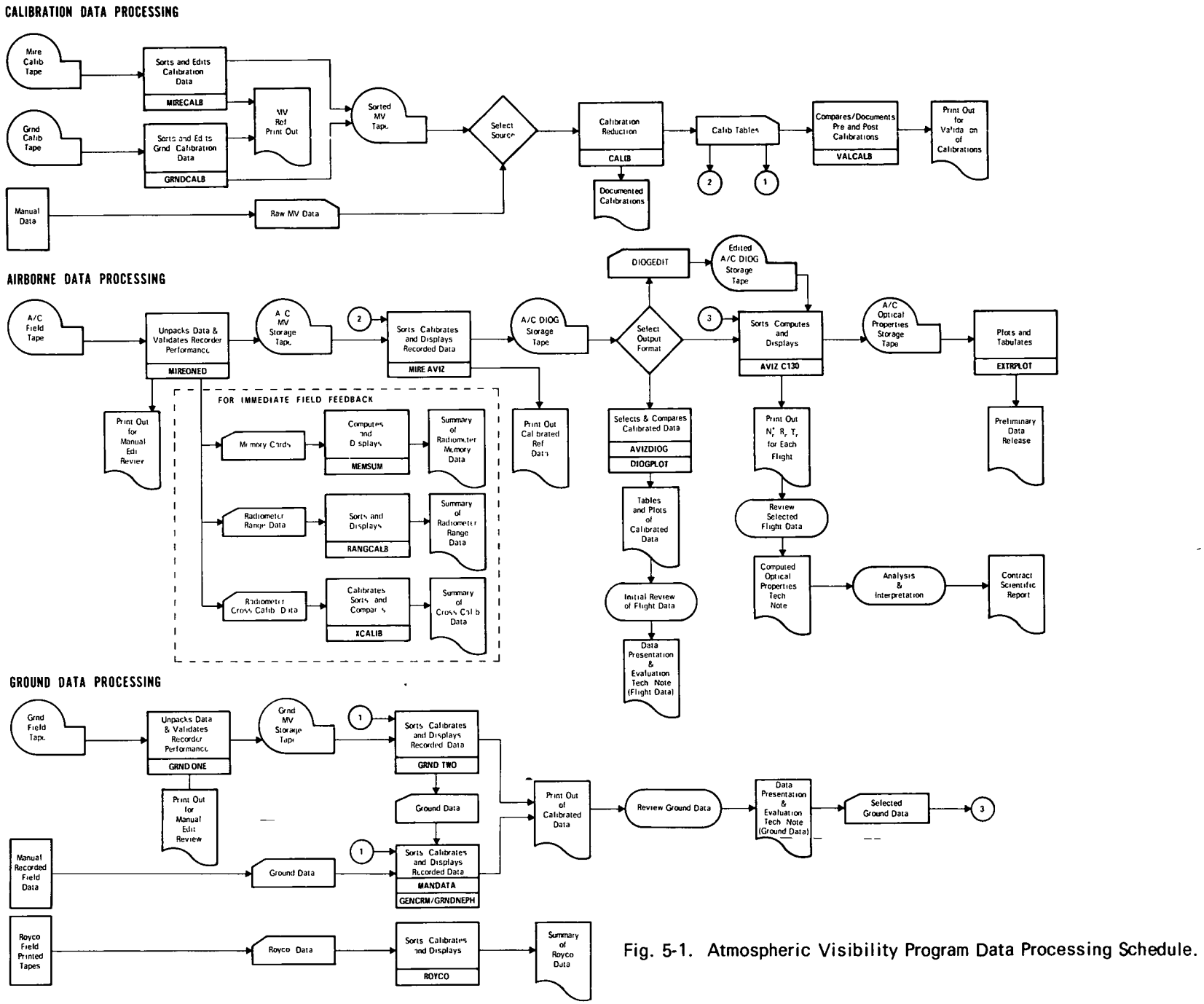

Fig. 5-1. Atmospheric Visibility Program Data Processing Schedule.

5.1 AIRBORNE DATA

A complete description of each modification made to the computer routines used during this contract interval is beyond the scope of this report. Since many affected only the overall system speed and not the resultant computations or output formats, they would be of little interest to the general reader in any case. However, a few illustrative remarks describing several typical updates accomplished during the interval are not inappropriate and are included in the following paragraphs.

PROGRAM MIREONED

This routine directs the first pass of the raw field tape through the computer. It presents the experimentalist his first opportunity to inspect the results of his measurements. The basic performance of Program MIREONED is described in Duntley, *et al.* (1972a). Several updates implemented subsequent to the issuance of that report and related primarily to the generation of a quick look capability are discussed below:

1. Improved MEMSUM extraction. The memory radiance data for each entire flight are extracted and displayed. The average value and standard deviation of the in-flight memory radiance readings yield an immediate check on the performance of each radiometer system throughout the flight. This information is automatically formatted on card output for use by program MEMSUM and on printer output for return to the field team.

2. Improved XCALIB extraction. The radiance measurements made with the upper and lower hemisphere scanners and the equilibrium radiance telephotometer during the in-flight cross-calibration maneuvers are extracted and displayed. The early availability of these data not only aids in the validation of the overall system's performance, but also provides a realistic test for the quality of the predeployment absolute calibration data. This information is also available on cards for use by Program XCALIB and in printed format for use by the field team.

3. Improved RANGECALIB extraction. The radiance measurements made with each radiometer during each straight and level flight element are sorted for maximum and minimum values. These calibrated values enable a prompt evaluation of the entire radiometric data set. This subroutine provides data for early detection of radiometer malfunctions and operator blunders. If these preliminary data fail to indicate adequate overall quality, the flight data can be eliminated from future processing at a substantial savings in computer- and man-hours.

PROGRAM MIREAVIZ

This routine directs the second pass of the field data through the computer. It performs the bulk of the fully automatic processing associated with each set of flight data and is also described in Duntley, *et al.* (1972a). Several recently implemented updates which are related primarily to improving downstream utilization of the data are summarized below.

1. Improved data-flagging techniques to automatically identify offscale values. The flags have been devised to identify the degree of scale overshoot so that the analyst can extract interpretive insights from the character of these normally lost data points. In some exceptional cases

it is worthwhile to extrapolate a calibration curve to attempt a retrieval, even though the data must be assigned a lower level of confidence.

2. Added diagnostic storage tape as a standard output. This tape has a format containing selected calibrated and specially flagged data which lends itself to the highly stylized processing desired in the subsequent processing phases. This tape provides the input data to all subsequent computational routines and is thus formatted for efficient editing and fast turnaround. The efficient use of this diagnostic tape provides the basic capability for the stylized data presentations and evaluations which lead to the generation of scientific reports, such as Duntley, *et al.* (1972a and b).

5.2 GROUND-BASED DATA

The automatic processing of ground-based data during the past contract interval has been plagued by intermittent logical malfunctions within the data logger. As a result, the development of the software related to these data has been directed toward the handling of manually recorded data which have been converted to punched card format. This is at best a highly inefficient process, and minimal effort has been expended in pursuing it. Beginning with the Project METRO deployment in August 1971, the ongoing troubleshooting of the ground-based data logger began to result in more reliable operation. Consequently, with the availability of usable test and data tapes from this deployment, a renewed emphasis on programming for automatic processing was initiated. The data backlog from Project METRO is currently being prepared for publication, and the discussion of the data processing applied to these data will be included in that report.

5.3 DATA ANALYSIS FORMAT

With the exceptionally large data-gathering capability demonstrated by the airborne instrument system described in Duntley, *et al.* (1970) and Duntley, *et al.* (1972a and b) and with the increasingly rapid data processing capability generated by the continued implementation of the scheme illustrated in Fig. 5-1, it became apparent very quickly that the data analyst was becoming the operational bottleneck. In an effort to simplify the data analysis procedures and thus shorten the elapsed time between raw data acquisition and interpreted data publication, a scheme for processing in stylized stages was evolved. The scheme was designed around two simplifying rules:

1. Handle the data in small independent units. Each data flight therefore has been specified as a basic unit and it retains its identity throughout the process.

2. Stylize both the processing and the evaluation procedures to an exceptionally high degree. This rigid formatting readily lends itself to machine-made comparisons of selected measured data versus predefined standards of acceptability.

Implementation of the basic data analysis scheme has been formalized through the generation of two in-house working documents identified as Technical Notes, for each data flight.

The output from Program AVIZDIOG generates tables and plots of calibrated data representing every measurable acquired during a data flight. These tabular data, without adjustment or editing, are compared against predefined standards of acceptability. The comparisons are made both by machine and by the engineering analyst. Each flight processed is subjected to exactly the same set of comparative tests. Subsequent to the completion of these tests the working document describing the flight and its data is prepared. This stylized in-house document contains a complete description of the data flight. It includes location maps, meteorological reports, procedural notes, and equipment assignments in addition to the output from AVIZDIOG and its evaluation. The data evaluation includes the recommendation for or against further processing of the subject data flight. The in-house document is identified as the Data Presentation and Evaluation Note. It is not reproduced for distribution, but is retained as the first indepth look at the experimental data. This Note provides a standardized source of information which allows any Visibility Laboratory scientific analyst to clearly and rapidly identify the basic quality of the flight data.

The data flights which adequately meet their diagnostic tests are scheduled for the second step of processing and interpretation. On the basis of the evaluations made at the Data Presentation level, technical editing, if necessary, is performed on the diagnostic storage tape by Program DIOGEDIT. This corrected and/or edited tape is now used as the input to Program AVIZC130.

The output from Program AVIZC130 generates tables and plots of computed optical properties similar to those reported by Duntley, *et al.* (1972a and b). These derived data are also compared against predefined standards of acceptability. At this level, the comparisons and interpretations are made by the scientific analyst. No comparisons are made by machine. Again, each flight that is processed to this stage is subjected to an identical set of comparative tests. However, at this point the analyst is free to include any additional objective or subjective analysis that he desires. Subsequent to the completion of these interpretations, the second working document related to the subject data flight is prepared. This second document includes the tables and plots of each computed optical property derived from the basic flight data and the analyst's item-by-item evaluation and interpretation. This second in-house document is identified as the Computed Optical Properties Note. It is not reproduced for distribution, but is retained as the final prepublication look at the experimental data.

When all of the data flights from any given field deployment have been processed to the point of being either rejected for poor quality or documented with a Computed Optical Properties Note, the data has reached the end of its rigorously stylized handling. At this point the entire deployment data set, represented by six to ten Computed Properties Notes, is reviewed, subjected to final scientific interpretation which includes peripheral studies and displays from other sources, and reformatted for submittal as a contract Scientific Report. The results of this general data analysis scheme are illustrated in Duntley, *et al.* (1972a and b).

Among the basic advantages of the step-by-step scheme described in the preceding paragraphs are the following.

1. Each data flight is judged on its own merit in a consistent, objective manner. The effort expended on each flight can be adjusted to remain commensurate with the data quality at each step in the procedure.

2. Preliminary evaluations and note preparations can be reliably and competently accomplished by machine and/or by junior level analysts.

3. Prior to publication preparation, the senior analysts have several well-defined intermediate landmarks at which they can inject corrections and/or updates to the data or evaluation techniques without disrupting the overall data schedule, a major consideration in an ongoing program.

6. DATA ACQUISITION SUMMARY

6.1 FIELD TRIP SUMMARY

The data acquired during the 3-year contract period were primarily daytime airborne measurements Nine field trips were made between November 1969 and August 1972 and a total of 79 flights made The locations, dates, and flights for each of the field trips are presented in Table 6-1 When dates are given without flight numbers, the reference is to the ground station site and the number of ground data sets Flight numbers which are not listed were assigned to flights during which no optical data were taken

6.2 DESCRIPTION OF FIELD TRIPS

HAVEN VIEW

The HAVEN VIEW field trip encompassed 74 days in April, May, and June 1970 During this time, there were 25 data flights and 20 ground-based data sets The field trip utilized four flight track locations one in the western Mediterranean Sea near the Balearic Islands, the second in north central Spain near Valladolid, the third in eastern Morocco southwest of Berguent, and the fourth in southern Germany near Memmingen The track locations are depicted in Fig 6-1 The ground station was located at the Memmingen Air Base near the Memmingen flight track The technical procedures for the HAVEN VIEW field trip are summarized in in-house Technical Note No 14

Balearic Islands. The six flights using the Balearic flight track started from Torrejon Air Base, Spain The flights were conducted over the Mediterranean Sea off the Balearic Islands One of the six flights, C-122 on 24 April 1970 was at night, during moonlight

Valladolid. The two flights using the Valladolid flight track also were initiated at the Torrejon Air Base in Spain The flights were conducted over land in the Valladolid/Leon plateau area in northern Spain The terrain was flat and cultivated, dry and brown Occasional patches of green appeared near rivers but they were the exception

Table 6-1

Field Trip Summary

Field Trip	Geographic Location	Track or Site Reference	Latitude	Longitude	Ground Elevation (meters)	Date Begin	Date End	Flight No.	Total No. Flights or Ground Sets
HAVEN VIEW	Western Mediterranean Sea	Balearic Islands	38 5° N	0 5 to 2 0° E	0	18 Apr 70	28 Apr 70	120 to 125	6
	Northern Spain	Valladolid	40.7° to 42.5° N	4.8 to 5.8°W	915	30 Apr 70	1 May 70	126 to 127	2
	Eastern Morocco	Kenitra	33.5° N	2.0 to 3.0°W	1220	6 May 70	8 May 70	128 to 130	3
	Southern Germany	Memmingen	48.0° N	9.9° E	629	19 May 70	7 Jun 70	131 to 144	14
	Southern Germany	Memmingen Air Base	48.0° N	10.2° E	629	4 May 70	7 Jun 70	–	20
ATOM	Central New Mexico	Stallion	33.3° N	106.5° W	1448	22 Oct 70	4 Nov 70	150 to 158	9
	Central New Mexico	Stallion	33.7° N	106 7° W	1450	22 Oct 70	4 Nov 70	–	9
SNOWBIRD	Northern Michigan	Green Bay	45.2° N	87.2° W	190	2 Mar 71	16 Mar 71	160 to 164, 167	6
	Northern Michigan	Mackinac	45.8° N	85.0° W	190	11 Mar 71	12 Mar 71	165 to 166	2
	Northern Michigan	Marinette	45.1° N	87.6° W	190	9 Mar 71	17 Mar 71	–	4

Table 6-1 (cont.)

Field Trip Summary

Field Trip	Geographic Location	Track or Site Reference	Latitude	Longitude	Ground Elevation (meters)	Date Begin	Date End	Flight No	Total No Flights or Ground Sets
LOCAL I	Southern California	Blythe/Yuma	33 2° N	114 9° W	305	29 Mar 71	30 Mar 71	170 to 171	2
	Southern California	San Clemente Island	32 7° N	117 9° W	0	31 Mar 71	1 Apr 71	172 to 173	2
DRUMMER BOY	Northern New York	Camp Drum	44 1° N	75 6° W	166	22 Apr 71	2 May 71	175 to 177	3
	Northern New York	Camp Drum	44 1° N	75 7° W	166	28 Apr 71	2 May 71	–	5
METRO	Southern Illinois	Track 1 Quincy/ Capitol	39 9° N	90 3° W	192	11 Aug 71	–	180	1
	Southern Illinois	Track 3 Vandalia	39 4° N	88 8° W	183	12 Aug 71	19 Aug 71	181,182-B, 185-B,186-B	4
	Southern Illinois	Track 4 Centralia	38 4° N	89 1° W	183	14 Aug 71	24 Aug 71	183-B,187-B, 188-B	3
	Southern Illinois	Track 7 Maples	37 8° N	91 5° W	305	13 Aug 71	23 Aug 71	182-A,183-A, 185-A,186-A, 187-A	5

Table 6-1 (cont.)

Field Trip Summary

Field Trip	Geographic Location	Track or Site Reference	Latitude	Longitude	Ground Elevation (meters)	Date Begin	Date End	Flight No	Total No. Flights or Ground Sets
METRO	Southern Illinois	Track 9: Hallsville	39 1° N	91 6° W	244	24 Aug 71	–	188-A	1
	Southern Illinois	Scott AFB	38 6' N	89 8° W	141	12 Aug 71	24 Aug 71	–	11
LOCAL II	Southern California	San Clemente Island	32 7° N	117 9° W	0	21 Oct 71	–	190	1
	Southern California	Blythe/Yuma	33 2° N	114.9° W	305	27 Oct 71	–	191	1
LOCAL III	Southern California	Blythe/Yuma	33.2° N	114.9° W	305	25 Jan 72	1 Feb 72	193, 197	2
	Southern California	Daggett	35.0° N	116.1° W	610	27 Jan 72	31 Jan 72	194 to 196	3
	Southern California	San Clemente Island	32.7° N	117.9° W	0	2 Feb 72	–	198	1
SENTRY	New Hampshire	Track 2: Concord	43 3° N	71 5° W	214	12 Apr 72	29 Apr 72	200 to 207	8
	New Hampshire	Concord	43.2°N	71.5° W	104	17 Apr 72	29 Apr 72	–	8

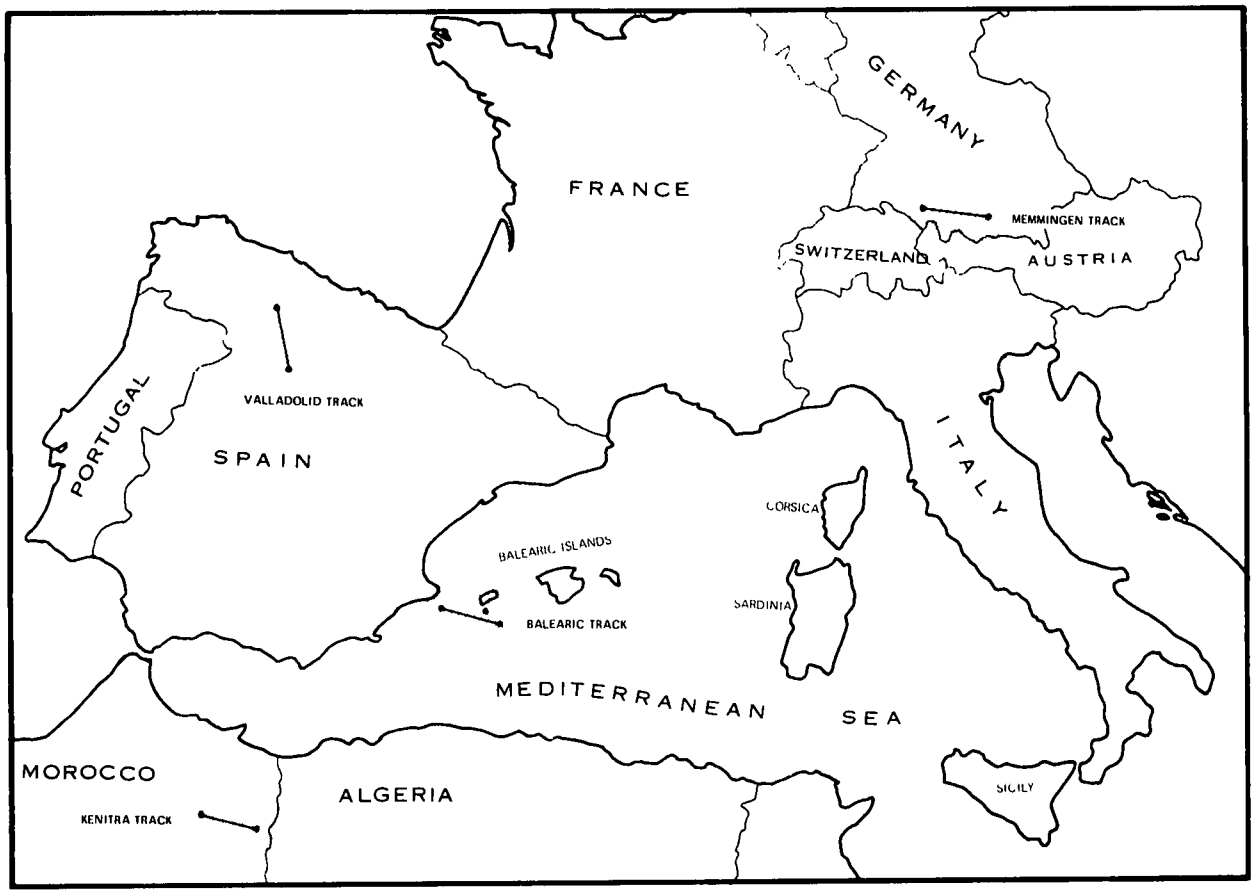

Fig. 6-1. Typical HAVEN VIEW Data Sites.

Kenitra. For the three flights using the Kenitra flight track, the airplane was based at the Kenitra Air Base in Morocco. The Kenitra track was over a high desert plateau. The terrain was typical sand and scrub.

Memmingen. There were 14 flights made using the Memmingen track. These flights were initiated from the Memmingen Air Base, Germany. The Memmingen track was green and heavily cultivated. Occasional large patches of dark forest interrupted the typically green terrain patterns. One of the 14 flights, Flight C-135 on 26 May 1970 was at night during starlight. The data for six of the daytime flights have been reported in Duntley, *et al.* (1972a). In-house Technical Note No. 28 through 34 and 38 through 43 document the Memmingen flights.

Memmingen Ground. The ground-based data station was situated at the Memmingen Air Base. One ground-based data set was taken at night during starlight on 26 May 1970. The daytime ground-based data are also reported in Duntley, *et al.* (1972a). In-house Technical Note No. 45 covers the Memmingen ground-based data.

ATOM

ATOM is an acronym for Atmospheric Optical Measurements. This 19-day field trip to central New Mexico occurred during the latter part of October and the beginning of November 1970. During the field expedition there were nine data flights and nine ground-based data sets. Data for six of the flights have been reported in Duntley, *et al.* (1972b). The technical procedures for the field trip are also summarized in in-house Technical Note No. 15.

Stallion. The ATOM flight track was at the northern end of the White Sands Missile Range as depicted in Fig. 6-2. Stallion Range Center is a radiosonde station near the flight track. The typical terrain was desert sand and low scattered brush. All nine flights used the same basic flight track. The flights initiated from Kirtland Air Base. In-house Technical Note No. 18, 19, 25, 26, 46 through 52, 54 through 57, and 59 document the ATOM flights.

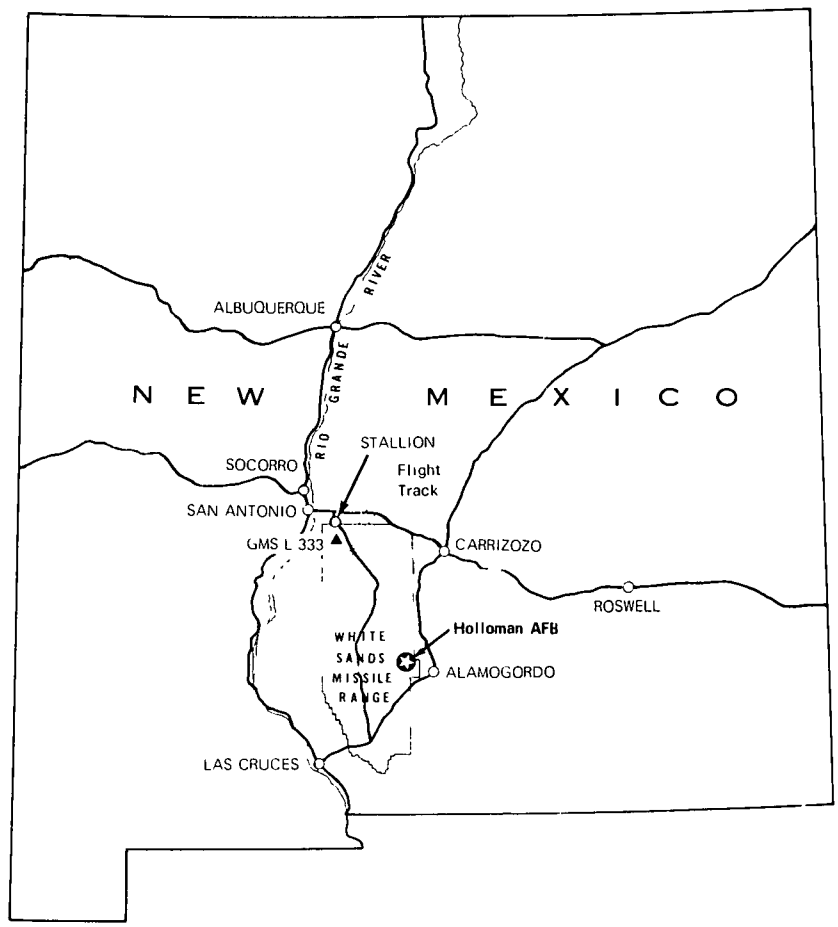

Fig. 6-2. Typical ATOM Data Sites.

Stallion Ground. The ground-based data station was located at Stallion as depicted in Fig. 6-2. The ground-based data for all but 30 October 1970 are reported in Duntley, *et al.* (1972b). The data for 30 October 1972 will be presented in Section 7. In-house Technical Note No. 16 and 21 cover the ATOM ground-based data. ATOM is the first field trip where the contrast reduction meter was added to the ground instrumentation.

SNOWBIRD

SNOWBIRD was a 19-day field trip to northern Michigan. The aircraft operated out of Kincheloe Air Base near Sault Ste. Marie, Michigan. Between 2 March and 17 March there were eight successful data flights and four ground-based data sets. The track locations and ground-station site at Marinette are depicted in Fig. 6-3. The same filters were used as for the previous two field trips but the code designations on Filters 4 and 5 were reversed for the SNOWBIRD and ensuing field trips. The technical procedures for the SNOWBIRD trip are summarized in in-house Technical Note No. 20.

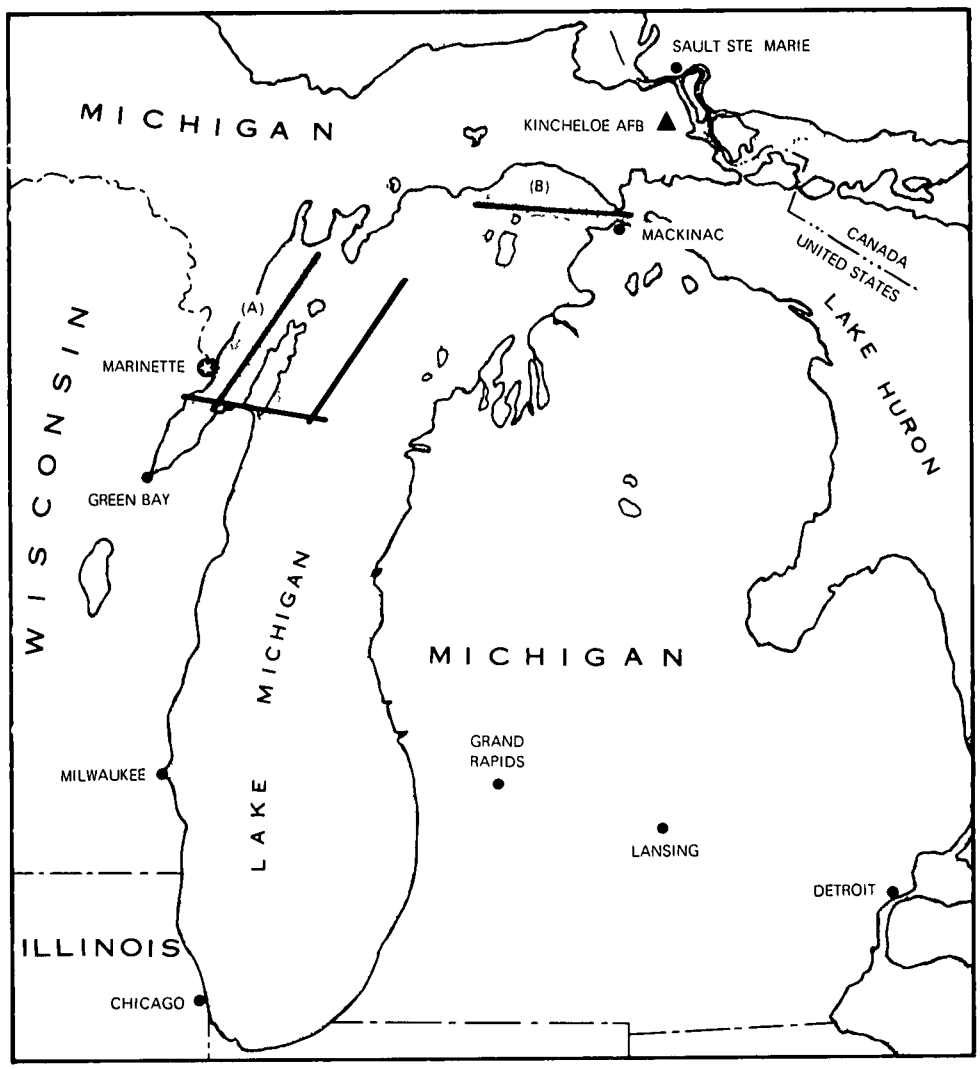

Fig. 6-3. Typical SNOWBIRD Data Sites.

Green Bay (A). There were six flights utilizing the Green Bay flight track at the northwestern edge of Lake Michigan This track was close to the ground station site at Marinette. The terrain beneath was snow-covered ice. For the portions of the flight track which extended out over Lake Michigan, the underlying water was not frozen and was clear of ice.

Mackinac (B). There were two flights utilizing the Mackinac flight track at the northeastern end of Lake Michigan. The terrain beneath was snow-covered ice.

Marinette Ground. The ground station contained only the contrast reduction meter (CRM). It was located on the western edge of Green Bay. The terrain beneath the CRM was hard-packed snow and showed many vehicle tracks

LOCAL I

Four flights local to the Visibility Laboratory location in San Diego, California, were made on four days at the end of March and beginning of April 1971. The airplane operated out of Lindbergh Field and Miramar Naval Air Station. No ground station data were taken during this period There were two flight tracks utilized one over land in the Blythe/Yuma area and one over water. The flight tracks are shown in Fig. 6-4. The XCAL flight element for cross-calibrating the upper hemisphere scanner, the lower hemisphere scanner, and the equilibrium radiance telephotometer was initiated during the LOCAL I flights and was used for all ensuing field trips. The technical procedures for LOCAL I are described in in-house Technical Note No. 53.

Blythe/Yuma. The flight track for two of the flights was between Blythe and Yuma near the southeastern corner of California This was a low desert area. The terrain was typically sand hills and low brush

San Clemente Island. Two of the flights utilized the track west of San Diego over the water near San Clemente Island. For both of the flights the sea was relatively calm

DRUMMER BOY

A 17-day field trip to northern New York was made during the latter part of April and early May 1971. The aircraft operated out of L. G Hanscom Field in Bedford, Massachusetts. Three flights were made and five ground-based data sets measured during the field trip The flight track was near Camp Drum where the ground station was located (see Fig 6-5) The technical procedures for DRUMMER BOY are outlined in in-house Technical Note No 22

Camp Drum. The flight track was along an east/west line slightly north of Watertown, New York. The terrain beneath was wooded low hills and cultivated fields. Although the Boston area was clear enough for takeoff, for two of the flights, C-175 and C-177, the Camp Drum area was below minimums for VFR flight so no data were taken. Since the airborne nephelometer malfunctioned during Flight C-176, there are no airborne data from the DRUMMER BOY field trip from which beam transmittance, path radiance, and path reflectance can be derived. In-house Technical Note No 23 describes the status of the airborne data for this field trip.

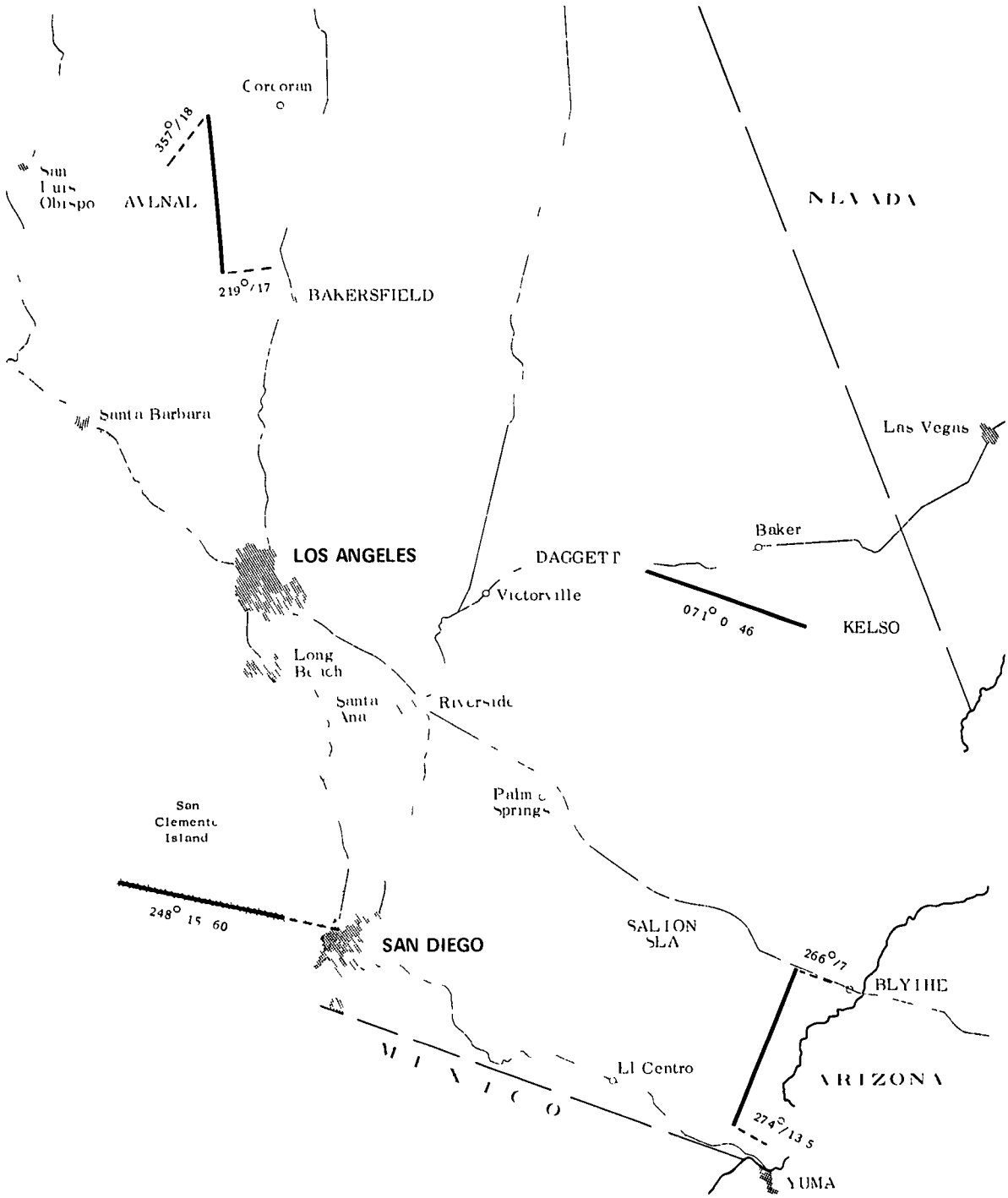

Fig 6-4. Typical LOCAL Data Sites

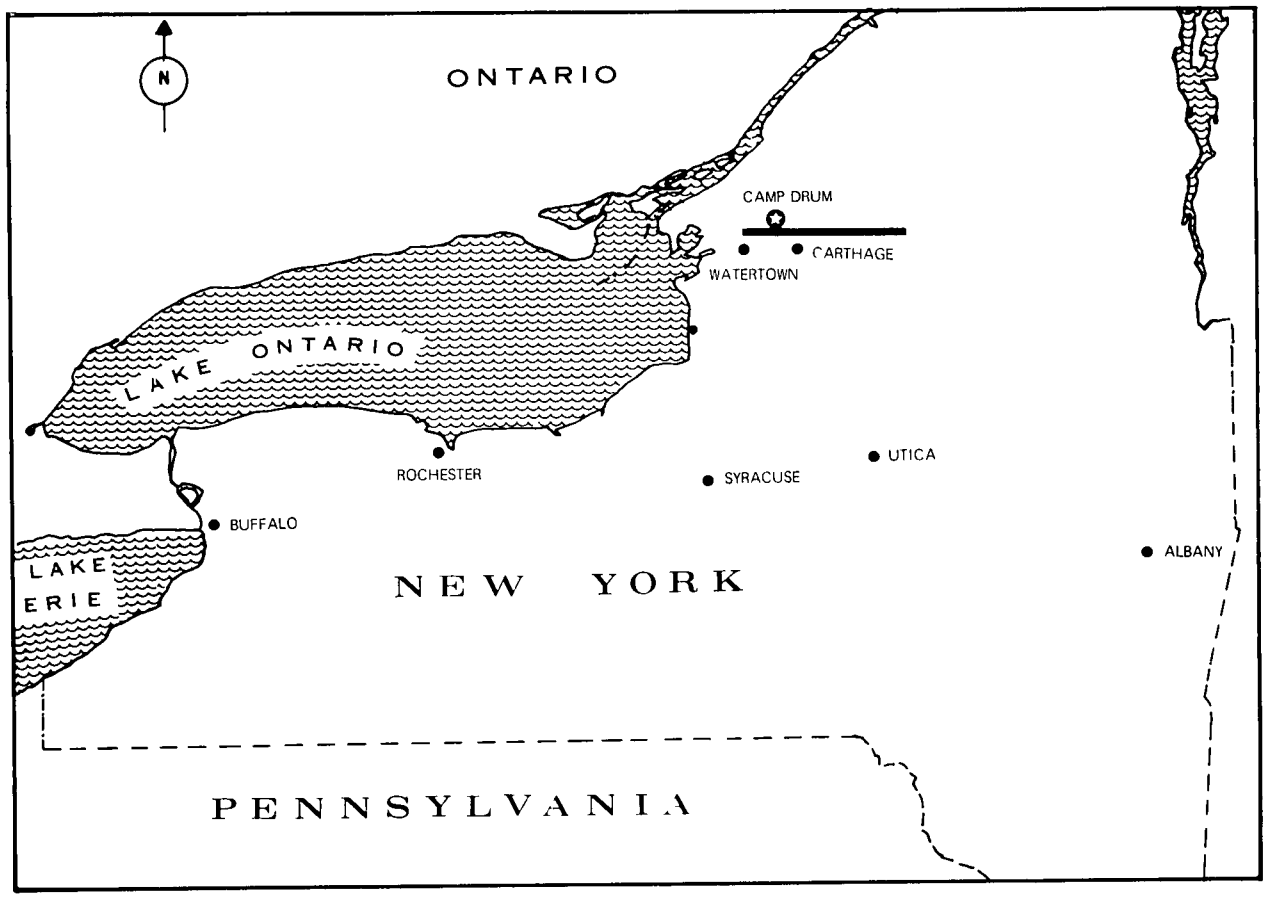

Fig 6-5 Typical DRUMMER BOY I Data Sites.

Camp Drum Ground. The ground station utilized only one instrument, the contrast reduction meter. Two site locations on Camp Drum were used In both localities the terrain was described as flat-lying grass, golden in appearance The ground data are presented in in-house Technical Note No 27

METRO

A 15-day field trip was made to southern Illinois in August 1971 The airplane operated out of Scott Air Base. There were 14 data flights and 11 ground-based data sets The St Louis area was selected in order to conveniently sample the optical properties both upwind and downwind of a major inland city. Additional benefit was derived from simultaneous operation with Program METROMEX (Metropolitan Meteorological Experiment), a long term multi agency cooperative research program operating in the St Louis area. Five out of nine designated track locations surrounding the city were used during the field trip The tracks are depicted in Fig 6-6. The ground station was situated at Scott Air Base, also shown in Fig. 6-6 The technical procedures for METRO are outlined in in-house Technical Note No 35

Track 1: Quincy/Capitol. Only the first flight utilized the track directly north of St. Louis. The terrain was cultivated farm area

Track 3: Vandalia. There were four flights on Track 3 northeast of St. Louis. The terrain was flat, highly cultivated farm land with multiple small fields.

Track 4: Centralia. Three flights took place on Track 4 which was east-southeast of St. Louis. The terrain along this track was flat, highly cultivated farm land and small bodies of water.

Track 7: Maples. The track southwest of St. Louis had Maples at one end. Five flights used this track. The terrain was heavily wooded rolling hills.

Track 9: Hallsville. Track 9 which was northwest of St. Louis was used only during the last flight of the field trip. The terrain was cultivated farm area with small fields and woodlands.

Scott Ground. The ground station was located at Scott Air Base which was closer to St. Louis than any of the flight tracks. A fully instrumented truck van was used containing instruments parallel to the airborne instruments in addition to the contrast reduction meter. The van was located on a mowed grassy field, which was generally dry and golden brown, with some slightly green areas.

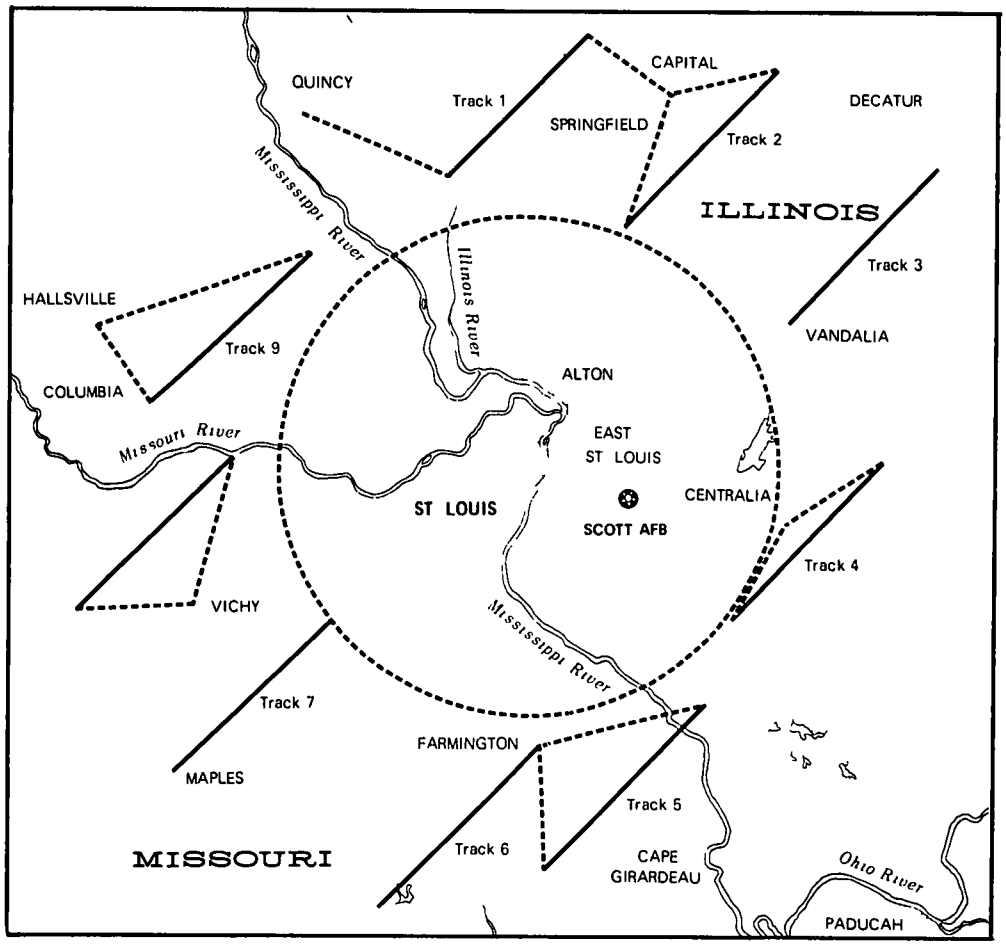

Fig. 6-6. Typical METRO Data Sites.

LOCAL II

Two flights were made in the local southern California area during October 1971. The airplane operated out of Lindbergh Field and Miramar Naval Air Station No ground data sets were measured during this period. Two track locations were utilized San Clemente and Blythe/Yuma (see Fig. 6-4). During these flights, a second mapping of the sky radiances with an additional three log neutral density filter was added to attempt to measure the apparent sun radiance and the solar aureole. This sun mode measurement by the upper hemisphere scanner was then used for all ensuing field trips The technical procedures for LOCAL II are described in in-house Technical Note No. 53.

San Clemente Island. One flight used the track west of San Diego over the Pacific Ocean. The sea was calm beneath the track.

Blythe/Yuma. One flight used the low desert track between Blythe and Yuma east of San Diego. The terrain was typically sand hill and low brush.

LOCAL III

Six flights were flown in the southern California area during the latter part of January and early February 1972. The airplane operated out of Lindbergh Field and Miramar Naval Air Station. No ground data sets were measured. Three track locations were utilized Blythe/Yuma, Daggett, and San Clemente (see Fig 6-4) These flights initiated the use of the new pattern of scanning the sky and terrain The new pattern no longer is a spiral upward to zenith but sweeps in azimuth at set constant zenith angles It is also a slower pattern which should add to data reliability The technical procedures for LOCAL III are contained in in-house Technical Note No 53.

Blythe/Yuma. Two flights utilized the track east of San Diego between Blythe and Yuma The terrain was a low desert area, typically sand hills and low brush

Daggett. Three flights used a track north of San Diego between Daggett and Kelso This is a high desert area comprised of sandy washes and low brush

San Clemente Island. The last flight was over the ocean west of San Diego. The sea was calm with light chop.

SENTRY

A 30-day field trip was made in April 1972 to central New England The airplane operated out of L G Hanscom Field, Bedford, Massachusetts There were eight successful flights and ground data sets Only the primary track near Concord, New Hampshire, was used The ground station also operated from the outskirts of Concord (see Fig 6-7). The technical procedures for SENTRY are described in in-house Technical Note No 58

Concord. This east/west track lies between Concord and Lake Winnipesaukee. The terrain was typified by rolling hills, winter woods, and scattered frozen lakes. There were occasional small snow patches on the ground. There were no detectable green leaves on the trees.

Concord Ground. The fully instrumented truck van was located on the New Hampshire National Guard complex outside Concord, New Hampshire. The terrain surrounding the van was dry brown grass.

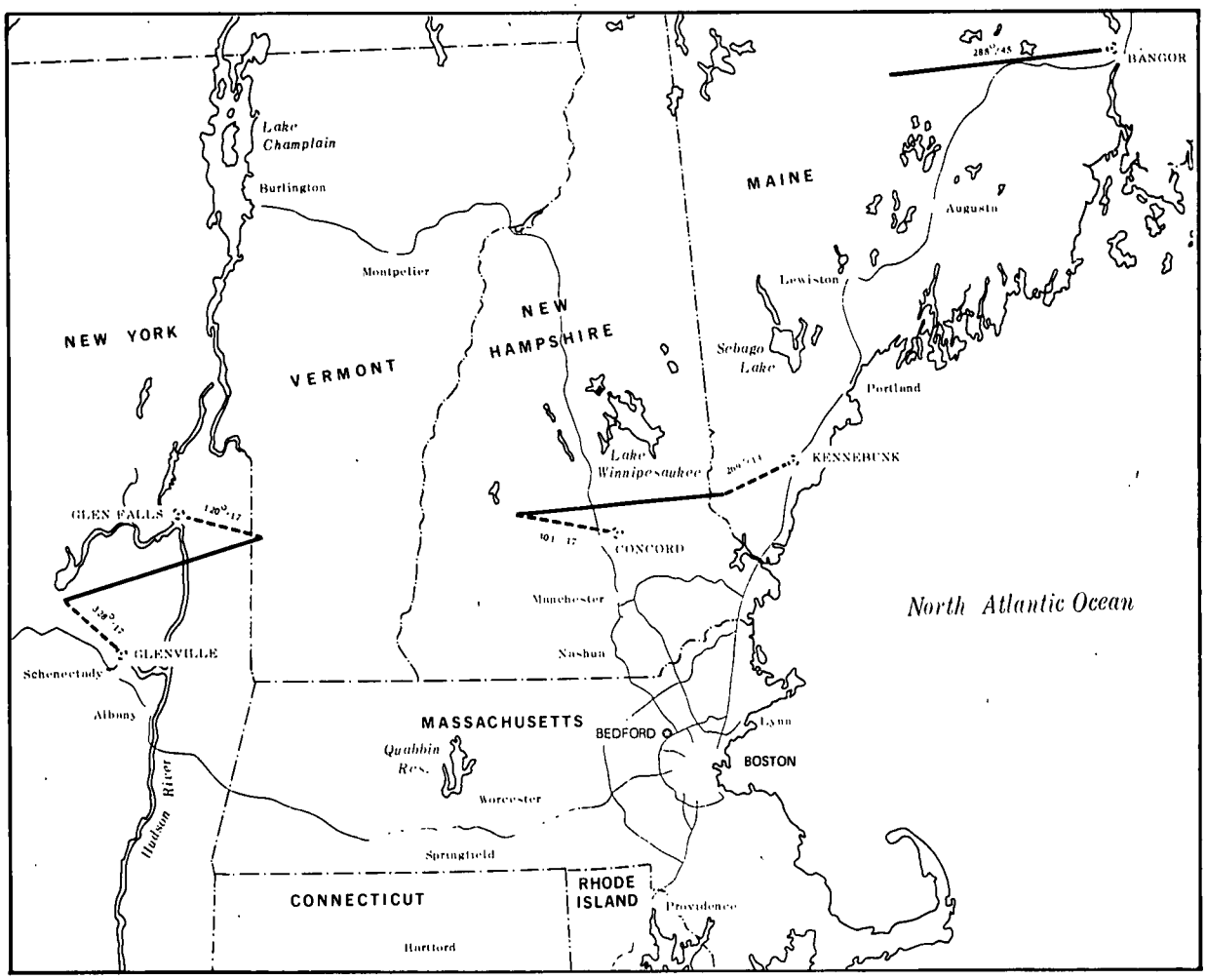

Fig. 6-7. Typical SENTRY Data Sites.

6.3 DATA BANK SUMMARY

The nine field trips described in Section 6.2 provide a data bank which can be used to derive atmospheric optical properties for the downward path of sight. An initial sorting of the flight data has been made to determine the number of flights which are sufficiently complete to warrant further processing. Data for three straight and level altitude runs plus the vertical profile data in each of three filters is the minimum requirement. A summary of these daytime flights is presented in Table 6-2. Of a total of 79 flights during the contract period, 64 are complete. In addition, there are seven daytime flights in the Puerto Rico area from the preceding project period, July 1969. These flights are sorted by latitude in Table 6-2 with the season and terrain briefly described.

The optical properties for 12 of the flights, 6 in Germany and 6 in central New Mexico, have been reported in Duntley, *et al.* (1972a and b). The METRO flights are currently being processed. Ten METRO flights are of sufficient data quality to warrant derivation of the optical properties for the downward path of sight. The METRO total scattering coefficient data will be described briefly in Section 7.

Table 6-2

Available Data Bank of Daytime Data

Latitude	Season	Terrain	Field Trip	Geographical Location	No. Complete Flights
48° N	May, June	green pasture	HAVEN VIEW	Southern Germany	10
45.5° N	Mar	snow, ice	SNOWBIRD	Northern Michigan	4
43.3° N	Apr	rolling hills, wooded	SENTRY	New Hampshire	8
41.5° N	Apr, May	dry range	HAVEN VIEW	Northern Spain	2
38.5° N	Apr	ocean	HAVEN VIEW	Western Mediterranean	4
38.5° N	Aug	cultivated farm	METRO	Southern Illinois	14
35.0° N	Jan	desert	LOCAL III	Southern California	3
33 5° N	May	high desert	HAVEN VIEW	Eastern Morocco	3
33.3° N	Oct, Nov	high desert	ATOM	Central New Mexico	7
33.2° N	Mar	low desert	LOCAL I	Southern California	2
33.2° N	Oct	low desert	LOCAL II	Southern California	1
33.2° N	Jan, Feb	low desert	LOCAL III	Southern California	2
32.7° N	Mar, Apr	ocean	LOCAL I	Southern California	2
	Oct	ocean	LOCAL II	Southern California	1
	Feb	ocean	LOCAL III	Southern California	1
18° N	Jul	ocean	TORTUGUERO	Puerto Rico	7

7. SELECTED COMPARATIVE DATA

Daytime atmospheric optical data for 12 flights were reported in Duntley, *et al.* (1972a and b). Project HAVEN VIEW flights were reported in Duntley, *et al.* (1972a) and Project ATOM flights in Duntley, *et al.* (1972b). The data included irradiance upon a horizontal plane surface, directional reflectance of terrain, total volume scattering coefficients, atmospheric beam transmittance, path radiance, and path reflectance. The data were derived for downward-looking paths of sight inclined at seven zenith angles between 93 and 180 degrees. A summary of the flights for which data were reported is given in Table 7-1. In the fourth column of Table 7-1 labeled Sky Near Sun, "clear" indicates that the apparent sun radiance was calculated assuming a clear sky above the highest flight altitude and no change except density in the aerosol content above that altitude. "Cloud" indicates that the highest measured sky radiance was accepted as the apparent sun radiance since there were clouds above the highest flight altitude.

Additional data from Project ATOM, as well as selected scattering coefficient profiles from Project METRO, both previously unpublished, are presented in the following sections.

7.1 ATOM CRM DATA FOR 30 OCTOBER 1970

Contrast reduction meter data from early morning until early afternoon were taken during Project ATOM on 30 October 1970. Since these data were not included in the ATOM report, Duntley, *et al.* (1972b), they are presented here. The contrast reduction meter and the theory and equations used to compute the path radiance and path reflectance from the contrast reduction meter measurements are described in full in Section 3 of Duntley, *et al.* (1972b) and will not be repeated here.

Data are presented in tables of:

Irradiance

Vertical Beam Transmittance Earth-to-Space

Vertical Path Radiance Earth-to-Space

Vertical Path Reflectance Earth-to-Space

In each table, the data are presented chronologically and by filter, with the filters in order of increasing mean wavelength. Note that Filter 6, a broad band optical filter with a mean wavelength of 532 nanometers, has been included although airborne data were limited to Filters 2, 5, 3, and 4. (Refer to Fig. 1-1 for further details on the spectral responses of the filters).

Table 7-1

Published Flight Data Summary

Field Trip	Flight No	Date (1970)	Sky Near Sun	Filters	Sun Zenith Angle (degrees) Start	Transit	End	Maximum Flight Altitude (meters) AGL
HAVEN VIEW	C 134	25 May	cloud	2,6,5 3	50 6	–	61 7	2460
	C 137	28 May	clear	2,6,5,3	44 8	–	55 1	2490
	C 138	29 May	clear	2 6,5,3	42 6	–	29 7	4920
	C 139	3 Jun	cloud	2,6,5,3	31 3	–	44 8	4830
	C 142	6 Jun	clear	2,6,5,3	42 7	–	30 2	4950
	C 143	6 Jun	cloud	2,6,5 3	41 8	–	58 9	4980
ATOM	C 151	24 Oct	clear	2 5,3	68 8	–	55 3	4425
	C 152	26 Oct	clear	2,5,3	57 9	–	49 5	4495
				4	46 3	–	47 9	4495
	C-154	28 Oct	clear	2,5,3	63 2	–	52 6	4375
				4	47 1	46 9	48 3	4375
	C-155	30 Oct	clear	4	61 0	–	53 7	4371
				2,5,3	50 7	47 6	47 6	4371
	C 157	3 Nov	clear	2,5,3	54 7	–	49 2	4374
				4	49 5	–	52 4	4374
	C 158	4 Nov	clear	2,5 3	61 2	–	52 0	4308
				4	49 3	49 2	50 0	4308

Users should be aware that regardless of the display format, the data values are valid to, at best, only three significant figures

IRRADIANCE

The downwelling irradiance H(o,d) measured by the contrast reduction meter on 30 October 1970 is presented in Table 7 2 The radiometer data for Filter 5 (pseudo-photopic) have been corrected to units of lu/m^2 (lux) and are given in Column 3

Table 7-2

Downwelling Irradiance Measured by the Contrast Reduction Meter on 30 October 1970 during Project ATOM

Time GMT	Sun Zenith Angle	Photopic (lu/m²)	Irradiance (w/m² μm) Filter 2 Blue	Filter 6 S-20	Filter 5 Psd-Phot	Filter 3 Red	Filter 4 N.I.R.
1335	86.8	2.78E+03	4.43E+01	4.37E+01	3 88E+01	3.78E+01	3.81E+01
1400	81.2	1.20E+04	1.75E+02	1 75E+02	1 67E+02	1.58E+02	1.52E+02
1430	76.3	1.97E+04	2 98E+02	2 73E+02	2 75E+02	2 44E+02	2.11E+02
1500	70.9	3.27E+04	4.92E+02	4 44E+02	4.56E+02	3.85E+02	3.26E+02
1530	66.6	3.50E+04	5.26E+02	4 76E+02	4 88E+02	4.12E+02	3.49E+02
1600	61.2	4.27E+04	6.49E+02	5.81E+02	5 95E+02	5.06E+02	4.21E+02
1630	56.8	5.05E+04	7.57E+02	6.65E+02	7.03E+02	5.89E+02	4.85E+02
1700	53.6	5.48E+04	8.20E+02	7.47E+02	7.64E+02	6 40E+02	5.29E+02
1730	50.5	5.82E+04	8.82E+02	7.68E+02	8.11E+02	6.80E+02	5.57E+02
1800	48.9	5.99E+04	8.97E+02	8.06E+02	8.34E+02	6.97E+02	5.73E+02
1830	47.1	6.06E+04	9.13E+02	7.95E+02	8.44E+02	7.03E+02	5.80E+02
1900	47.2	6.14E+04	9.17E+02	8.16E+02	8.55E+02	7.12E+02	5.88E+02
1930	49.0	6.22E+04	9.29E+02	8.27E+02	8.66E+02	7.22E+02	5.96E+02
–	51.5	5.78E+04	8.65E+02	7.89E+02	8.06E+02	6.75E+02	5.46E+02

VERTICAL BEAM TRANSMITTANCE EARTH-TO-SPACE

The contrast reduction meter determines earth-to-space beam transmittance based upon the ratio between a pre-established value of inherent solar radiance and a measurement of apparent solar radiance. The ratio is not corrected for small angle forward scattering due to historical evidence that, for atmospheres clear enough to adequately image the solar disk within the device, the aureole radiance 15 minutes off the limb is generally 1 percent or less of the center disk radiance.

A summary of the vertical path earth-to-space beam transmittance $T_{\infty}(\infty, 180^{\circ})$ measured on 30 October 1970 during Project ATOM is presented in Table 7-3. The bottom row of the table contains the computed values for a Rayleigh atmosphere, establishing an upper limit against which the measured values of beam transmittance may be judged.

Table 7-3

Earth-to-Space Vertical Beam Transmittance on
30 October 1970 during Project ATOM

Time GMT	Weather	Sun Zenith Angle (degrees)	Vertical Beam Transmittance				
			Filter 2	Filter 6	Filter 5	Filter 3	Filter 4
1335	Clear	86 8	0.806	0 878	0.867	0 903	0.922
1400	Clear	81 2	0.764	0.822	0.819	0.859	0 874
1430	Clear	76 3	0 734	0.786	0 790	0.827	0.835
1500	Clear	70 9	0 690	0 740	0 743	0 780	0.786
1530	Clear	66 6	0.669	0.713	0 727	0 766	0.757
1600	Clear	61.2	0.643	0 692	0 702	0 735	0 729
1630	Clear	56.8	0.617	0.673	0 683	0.718	0 704
1700	Clear	53 6	0.603	0.654	0.669	0.698	0 686
1730	Clear	50.5	0.577	0.640	0 652	0 688	0.656
1800	Clear	48.9	0.576	0.633	0.655	0 674	0 659
1830	Clear	47 1	0.565	0 616	0 635	0 673	0 644
1900	Clear	47.2	0 571	0.629	0 637	0 680	0.646
1930	Clear	49.0	0 583	0.639	0 652	0 683	0.656
–	Clear	51.5	0 586	0 651	0.659	0.697	0.668
Rayleigh Limit for each Filter			0 84	0 87	0 91	0.95	0.97

VERTICAL PATH RADIANCE EARTH-TO-SPACE

The earth-to-space vertical path radiance $N^*_\infty(\infty,180°,0°)$ for the downward-looking path of sight is a derived quantity, computed from selected measurements of apparent sun and sky radiances. A summary of these computed values is presented in Table 7-4.

VERTICAL PATH REFLECTANCE EARTH-TO-SPACE

Earth-to-space vertical path reflectance $R^*_\infty(\infty,180°,0°)$ is presented in Table 7-5. The path reflectance is computed from the values of path radiance, beam transmittance, and total downwelling irradiance previously presented in Tables 7-4, 7-3, and 7-2, respectively. This property is dimensionless.

Table 7-4

Vertical Path Radiance Earth-to-Space on
30 October 1970 during Project ATOM

Time GMT	Sun Zenith Angle (degrees)	Vertical Path Radiance ($w/\Omega\, m^2\, \mu m$)				
		Filter 2	Filter 6	Filter 5	Filter 3	Filter 4
1335	86 8	6.06	4.09	3.70	2.28	1.40
1400	81.2	11 4	6 47	6.05	3.00	1 75
1430	76 3	13 9	7.77	7.31	3 50	1.92
1500	70.9	14.8	8.36	7.76	3.61	1.98
1530	66.6	16 4	9.12	8.52	3.95	2.07
1600	61.2	17 7	9 67	9.15	4 29	2.19
1630	56.8	18 6	10.7	9.71	4 46	2.32
1700	53.6	18.7	10.4	9.75	4 61	2.35
1730	50.5	18.9	10.2	9 81	4 59	2.34
1800	48.9	19.0	10.8	9 95	4.63	2.39
1830	47 1	19.1	10 5	9 95	4.67	2.40
1900	47.2	19 1	10.6	10.0	4.59	2.40
1930	49.0	19.7	11.0	10.3	4.75	2.48
–	51.5	20.0	10.6	10.0	4.67	2.41

7.2 ANALYSIS OF CONTRAST REDUCTION METER DATA DURING ATOM FIELD TRIP

In the second scientific report of this contract period, Duntley, *et al.* (1972b), the contrast reduction meter data for near noon on 8 days of the ATOM field trip were presented in Section 7.5 and discussed in Section 8.2. The data from Section 7.1 for 30 October 1972 have been combined with the graphical data from Section 8.2 of Duntley, *et al.* (1972b) and are discussed below.

IRRADIANCE

The Project ATOM ground-level downwelling irradiance for the photopic Filter 5 can be compared to the ground-level values of Brown (1952). The illuminance values of Brown for unobscured sun and average cloud conditions have been converted to irradiance units and are presented as solid curves in Fig. 7-1.

The downwelling irradiances for Filter 5 as measured with the contrast reduction meter are depicted as separate data points The values previously reported in Duntley, *et al.* (1972b) for near noon on 8 separate days are given as circles. The data for 30 October from early morning to early afternoon are given as dots. The 30 October data show a general shift from equal and greater than the curve for unobscured sun in the early morning, to slightly below the curve for late morning and noon. They are all within the expected range (the unobscured sun curve is not a limit but an average).

Although the order of the filters by increasing mean wavelength is 2 (478 nanometers), 6 (532 nanometers), 5 (557 nanometers), 3 (664 nanometers), and 4 (765 nanometers), the irradiances for Filter 6 except during very early morning lie between those for Filters 5 and 3 Thus the irradiances H(filter) are in the order H(2) > H(5) > H(6) > H(3) > H(4) This inverted juxtaposition of the Filter 6 data for the ATOM field trip is not unexpected, since irradiances for these same filters computed from the daytime spectral irradiance values of Buchtemann and Hohn (1970) generally show this same spectral relationship. These computations and the resultant irradiances are described in Visibility Laboratory in-house Technical Note No. 44.

Table 7-5

Earth-to-Space Vertical Path Reflectance on
30 October 1970 during Project ATOM

Time GMT	Sun Zenith Angle (degrees)	Earth-to-Space Vertical Path Reflectance				
		Filter 2	Filter 6	Filter 5	Filter 3	Filter 4
1335	86 8	0 533	0 335	0 346	0 210	0 125
1400	81 2	0 268	0 141	0 139	0 0694	0 0414
1430	76 3	0 200	0 114	0 106	0 0545	0 0342
1500	70 9	0 137	0 0799	0 0720	0 0378	0 0243
1530	66 6	0 146	0 0844	0 0754	0 0393	0 0246
1600	61 2	0 133	0 0756	0 0688	0 0362	0 0224
1630	56 8	0 125	0 0751	0 0635	0 0331	0 0213
1700	53 6	0 119	0 0669	0 0599	0 0324	0.0203
1730	50 5	0 117	0 0652	0 0583	0 0308	0 0201
1800	48 9	0 116	0 0665	0 0572	0 0310	0.0199
1830	47 1	0 116	0 0674	0 0583	0 0310	0 0202
1900	47 2	0 115	0 0649	0 0577	0 0298	0 0198
1930	49 0	0 114	0 0654	0 0573	0 0303	0 0199
–	51 5	0 124	0 0648	0 0591	0 0312	0.0208

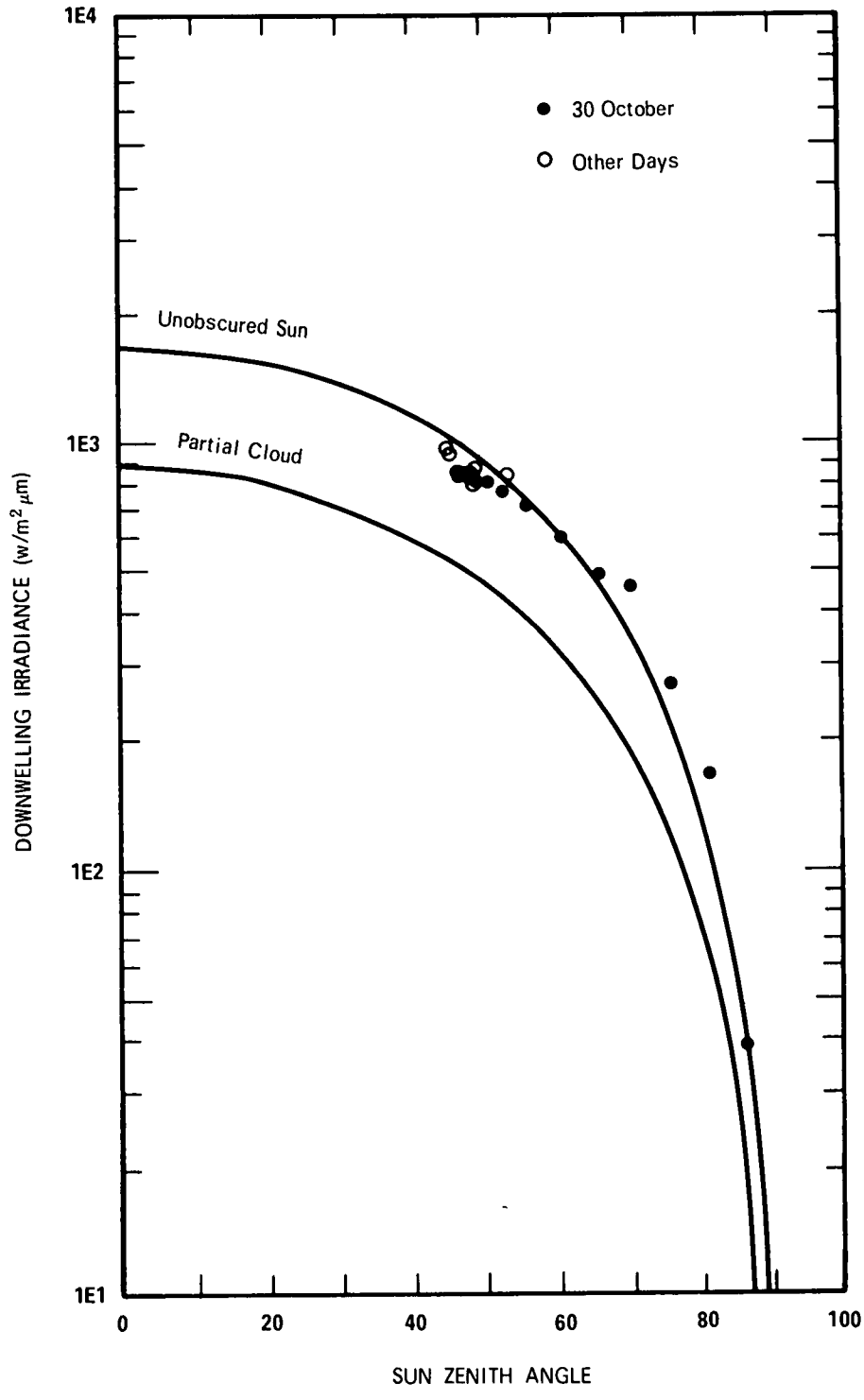

Fig. 7-1. Ground Level Downwelling Irradiance During ATOM Field Trip for Filter 5 (Pseudo-Photopic) as Compared to Brown (1952).

BEAM TRANSMITTANCE

Except in early morning, the space-to-earth vertical beam transmittance values as measured by the contrast reduction meter increased with wavelength, as expected, for Filters 2, 6, 5, and 3. Filter 4 (with a mean wavelength of 765 nanometers and a response area of 50 nanometers) is located in a portion of the spectrum dominated by the Fraunhoffer (A) oxygen absorption bands at 759.4 and 762.1 nanometers. Thus, the transmittance for Filter 4 is a product of the transmittance due to scattering and the transmittance due to absorption by 0_2. The vertical space-to-earth transmittance due to 0_2 absorption is sufficient to reduce the total transmittance for Filter 4 to less than the transmittance for Filter 3.

The slight anomalies in the filter order for the large sun zenith angle data may be due to the difficulties in measuring during early morning where small sun zenith angle changes with time have large effects on the relative airmass values used during data reduction. This might also account for the Filter 6 value at sun zenith angle 86.8 degrees appearing to be greater than the Rayleigh Limit.

In all spectral bands, the trend in transmittance is toward decreasing values as time approaches midday. The measures of exceptionally clear early morning air tend to corroborate the exceptionally clear nighttime data obtained from the AFCRL searchlight experiments during the ATOM field trip.

This trend in beam transmittance of decreasing values as time approaches midday is not uncommon. This same trend was consistently encountered during a field trip encompassing December 1964 through February 1965 near Laredo, Texas. The field trip was for the purpose of gathering data on the contrast transmittance of the atmosphere in the general area proposed for installation of a ground station for a visual acuity experiment conducted during Gemini Flights V and VII. The results of this trip are reported in Duntley, *et al.* (1968). The trend was consistent over the time period for measurements in three spectral regions: two narrow band filters with mean wavelengths of 448 and 656 nanometers and a broad band filter representing the photopic response, mean wavelength 560 nanometers. The contrast reduction meter data for the Laredo area are described in Visibility Laboratory in-house Technical Note No. 5.

PATH RADIANCE

The earth-to-space vertical path radiance values are derived from the contrast reduction meter measurements of apparent sun radiance and sky radiance. Since path radiance is defined as the light scattered into the path of sight, it can be expected to be inversely related to the mean wavelength of the filter, as is the scattering coefficient. The derived path radiances for all of the ATOM field trip display this expected spectral relationship.

The method of deriving path radiance from ground-based sky and sun radiance measurements is probably valid only for bandwidths where there is little or no absorption [see Gordon (1969) for implications of the no-absorption assumption]. Therefore, ground-based path radiance values for Filter 4 should be used with great caution, and the effect of absorption on the derivation methods used should be investigated.

The ground-based earth-to-space vertical path radiance values for Filter 5 (photopic) are presented graphically in Fig. 7-2 as a function of sun zenith angle. The solid curve represents a graphical average of over 350 photopic earth-to-space path radiance measurements made over a period of 5 years in various

geographical locations. The dashed curves are a rough estimate of the range of values (some fall beyond these dashed curves). The measurements summarized by these curves are described in Visibility Laboratory in-house Technical Note No. 5. The ground-based path radiances measured during the Fall of 1970 in central New Mexico are lower than the average but fit into the normal range of data.

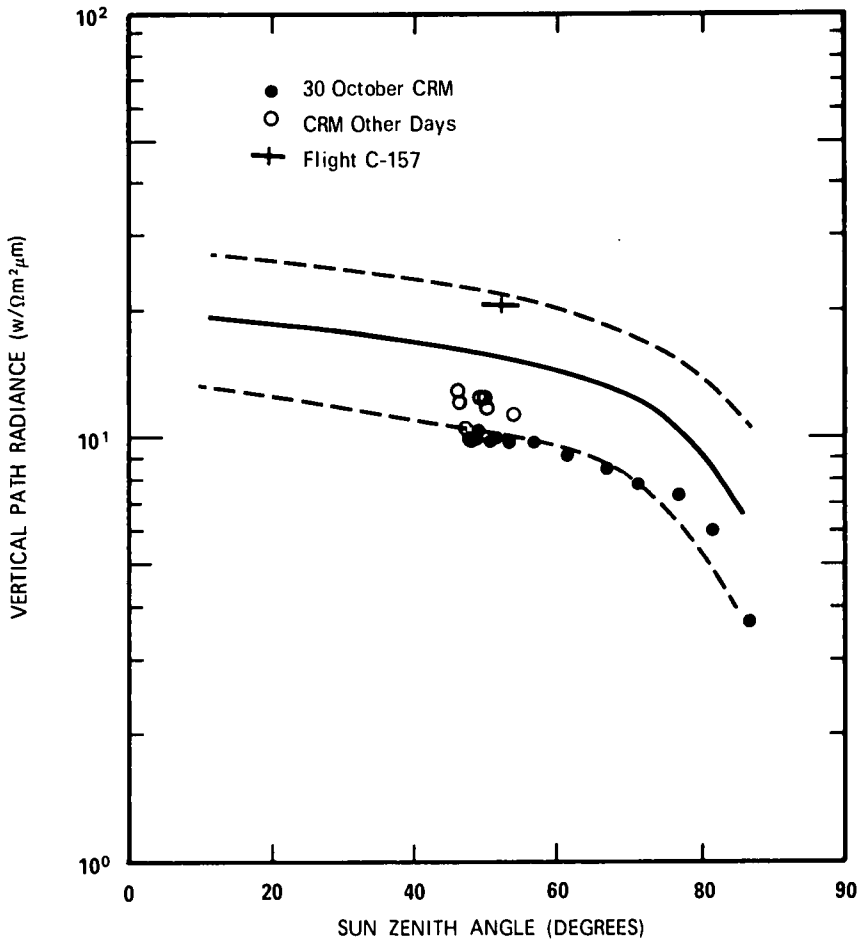

Fig. 7-2. Vertical Path Radiance on ATOM Field Trip for Filter 5 (Photopic) Compared to Graphical Average of Over 350 Earth-to-Space Measurements.

The airborne values of path radiance for earth to 4.5 kilometers should only be compared to the ground-based values for earth to space when the flights have comparable sun zenith angles and total beam transmittance values. Only one flight, Flight C-157, has Filter 5 data falling within that category. This airborne value for Filter 5 (Flight C-157) has also been graphed in Fig. 7-2. The horizontal length of the cross indicates the sun zenith angle span during the flight. This point also lies within the normal range of values, as indicated by the dashed lines, but is above the average.

PATH REFLECTANCE

The earth-to-space vertical path reflectance values are derived from the contrast reduction meter measurements of apparent sun radiance, sky radiance, and downwelling irradiance. The derived path reflectances display an inverse relationship to the mean wavelength of the filters, as expected on the basis

of previous measurements with various filters. However, great caution should be exercised in using the data from Filter 4 because of the domination of that portion of the wavelength band by oxygen absorption.

The ground-based earth-to-space vertical path reflectance values for the ATOM field trip for Filter 5 (photopic) are presented as a function of sun zenith angle in Fig. 7-3. The solid curve represents a graphical average of over 350 photopic earth-to-space vertical path reflectance values based on measurements made in various locations over a period of 5 years. The dashed curves are a rough estimate of the range of values. These curves are based on data graphs in Visibility Laboratory in-house Technical Note No. 5. The ground-based path reflectances measured in central New Mexico during the Fall of 1970 compare very well with the average curve and, except for three early morning values, easily fall within the normal range of values.

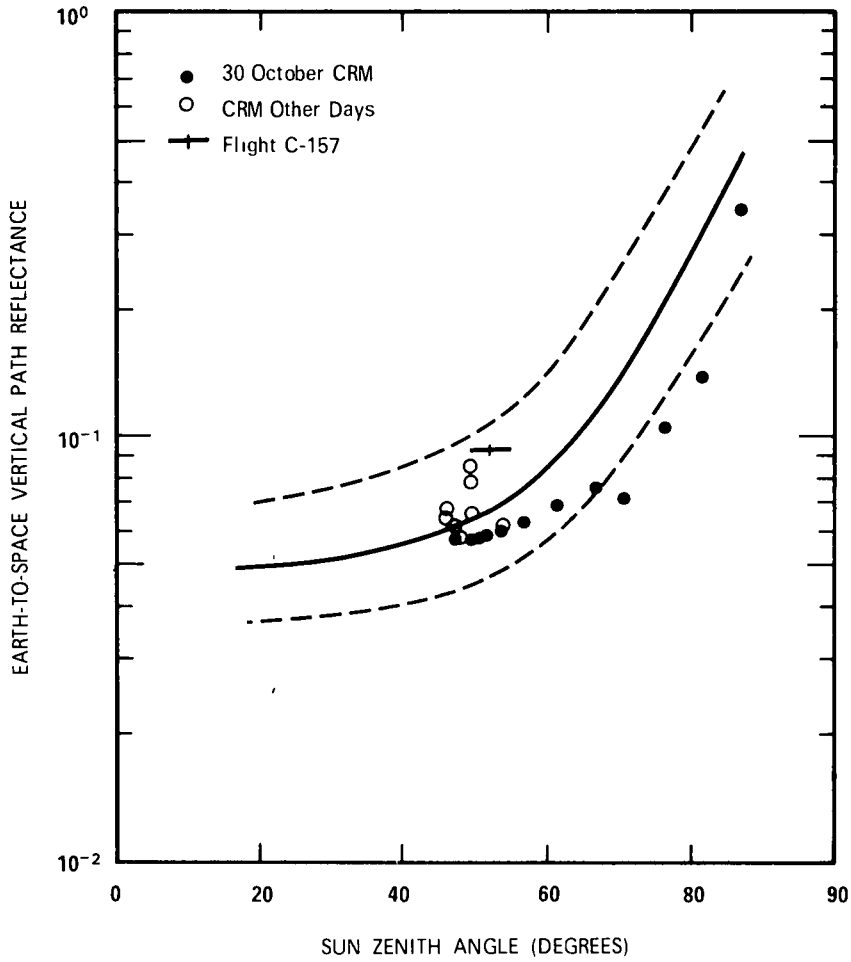

Fig. 7-3. Vertical Path Reflectance on ATOM Field Trip for Filter 5 (Photopic) Compared to Graphical Average of Over 350 Earth-to-Space Measurements.

The airborne value of path reflectance for the vertical path from earth to 4.5 kilometers for Flight C-157 is also depicted in Fig. 7-3. Although slightly higher than the ground-based values, it also lies well within the normal range of values.

7.3 TOTAL VOLUME SCATTERING COEFFICIENT COMPARISON

In order to compare the scattering characteristics of the various flights during a single field trip, the total volume scattering coefficient for the pseudo-photopic filter for all the flights has been plotted on one graph. This type of graph was prepared for each of three field trips: HAVEN VIEW, ATOM, and METRO.

HAVEN VIEW

The filter code was 5 for the pseudo-photopic filter during the HAVEN VIEW field trip. The graph for comparing the six HAVEN VIEW flights reported in Duntley, *et al.* (1972a) is presented in Fig. 7-4.

Characteristic of all six flights is a haze layer at the low altitudes (haze top between 1 and 2 kilometers) and a relatively clear area above the haze.

During all flights except Flight C-142 it was possible to take airborne data at altitudes often considerably lower than 0.5 kilometer. Thus, for most of the flights, the low altitude total scattering profile in the haze is well-documented. However, the shape of the total scattering profile between 0 and 1 kilometer for Flight C-142 was not documented and is merely an interpolation between the ground-based value and the lowest flight altitude near 1 kilometer. Therefore, the apparent difference in low altitude haze characteristics between Flight C-142 and the other flights is not a real measured difference but is due to the absence of data at the 0 to 1 kilometer altitudes for Flight C-142.

The lapse rate of the measured total scattering coefficients above the haze layer is less than the density lapse rate for all the flights with data above 3 kilometers (Flights C-139, C-142, and C-143). This was not expected. For Flight C-138, the total scattering coefficients for Filter 5 were extrapolated above 2.5 kilometers according to the density lapse rate. Thus, the difference in curve shape above 2.5 kilometers between Flight C-138 and the other three flights directly illustrates the difference in lapse rates between the scattering coefficient and the density.

ATOM

The graph of the total volume scattering data for Filter 5 for comparing the six ATOM flights was given as Fig. 8-2 in Duntley, *et al.* (1972b); it is reproduced below as Fig. 7-5.

During the ATOM field trip it was possible to take airborne data as low as 0.6 to 0.75 kilometer. Also, ground-based nephelometer data measured during the flights were available and were used for all but Flight C-151. Thus, for most of the flights, the low altitude total scattering profile is well-documented.

The lower altitude data, between ground level and 1.5 kilometers, are similar in magnitude for the six flights. Four of the flights (C-151, C-152, C-154, and C-155) change very little above 1.5 kilometers as well, whereas Flights C-157 and C-158 reach a haze top at about 2.5 kilometers and have a clearer area between 2.5 and 4.5 kilometers.

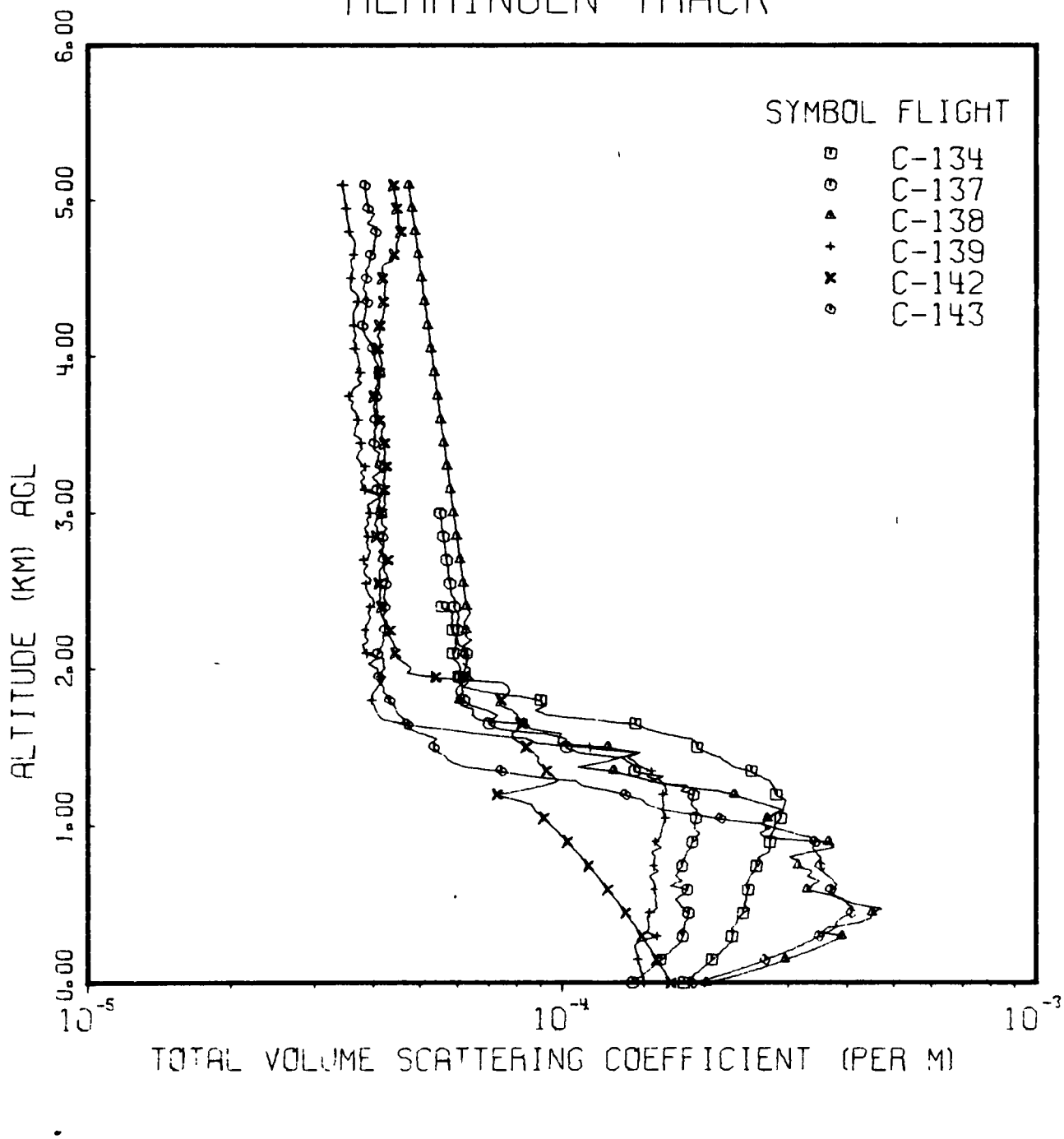

Fig. 7-4. Total Volume Scattering Coefficient for Filter 5 (Pseudo-Photopic) for the Six HAVEN VIEW Flights.

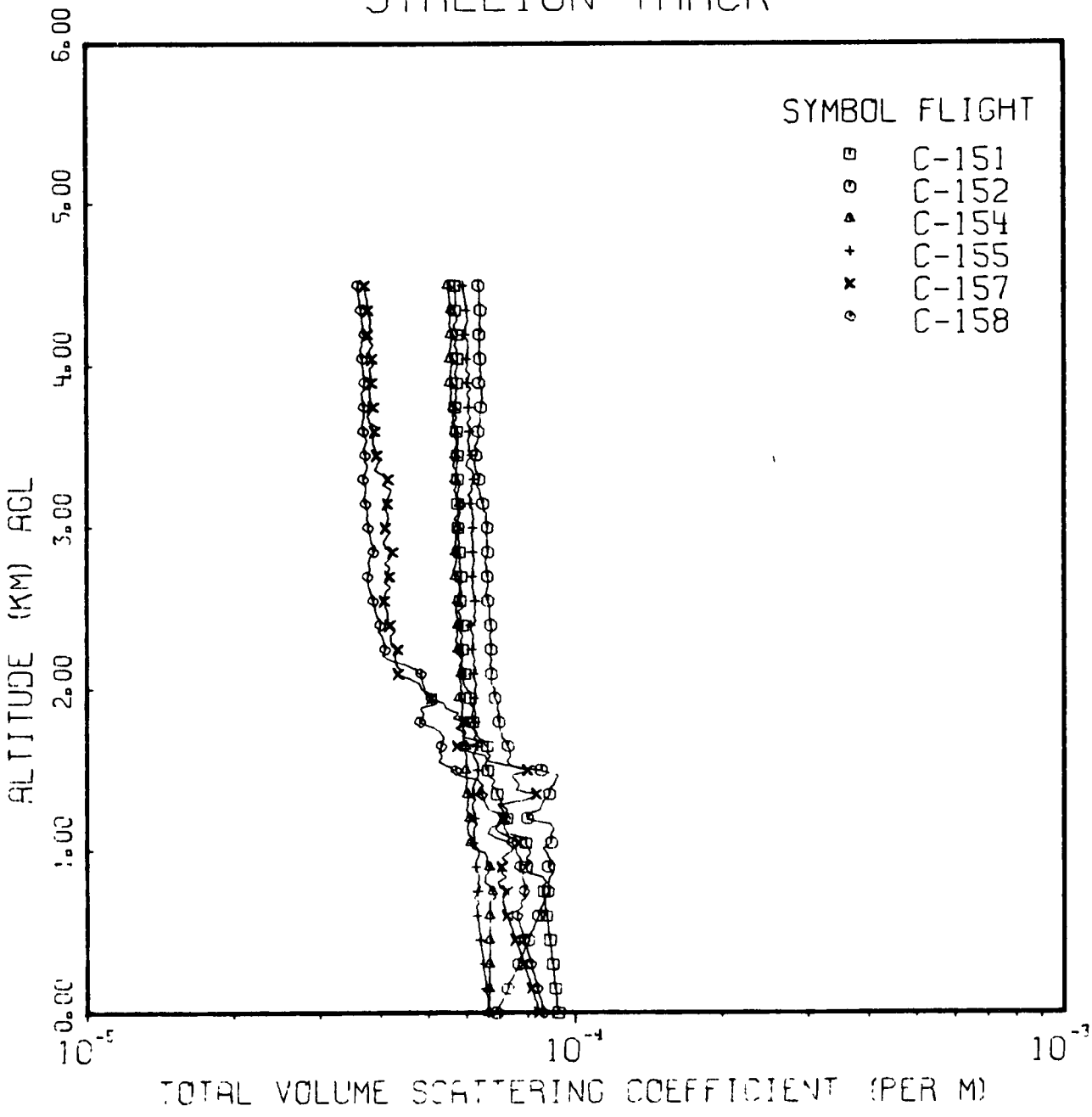

Fig. 7-5. Total Volume Scattering Coefficient for Filter 5 (Pseudo-Photopic) for the Six ATOM Flights.

Both the earth-to-space transmittances obtained from the contrast reduction meter and the flight descriptions indicate that the primary haze layer extends to at least 4.5 kilometers and that there is a clearer area somewhat above 4.5 kilometers for Flights C-151, C-152, C-154, and C-155.

The lapse rate of the measured total scattering coefficients at the higher altitudes between 2 and 4.5 kilometers for all the flights and from ground level to 4.5 kilometers for Flights C-154 and C-155 is less than the density lapse rate. This characteristic was also noted in the HAVEN VIEW high altitude data.

The scales for Fig. 7-4 and 7-5 have purposely been made equivalent so that the data for the two field trips could be inter-compared. All of the HAVEN VIEW data show a heavier haze layer than the ATOM data between ground and 1.5 kilometers. Above 2 kilometers, however, the data for Flights C-139, C-142, and C-143 are similar to the data for Flights C-157 and C-158. Also, above 2 kilometers the data for Flights C-134, C-137, and C-138 are similar to the data for Flights C-151, C-152, C-154, and C-155.

METRO

Although the total volume scattering coefficient data for the METRO field trip have not yet been reported, the data have been processed sufficiently so that comparison graphs could be made for 10 flights. These 10 flights are of sufficient data quality that path radiance and path reflectance values are derivable and planned for inclusion in a scientific report in the near future. A summary of these 10 flights is presented in Table 7-6.

The pseudo-photopic filter was coded as 4 during the METRO flights. The data for the 10 flights are presented in two graphs: Fig. 7-6 contains the data for the five flights using Flight Tracks 1, 3, 4, and 9; Fig. 7-7 contains all the flight data for Track 7. See Fig. 6-6 and Table 6-1 for further information on the flight track locations.

During all the flights except C-180 it was possible to take airborne data at altitudes less than 0.3 kilometers. However, the shape of the total scattering profile between ground and 1 kilometer for Flight C-180 was not documented. Figures 7-6 and 7-7 include only the airborne data since the ground-based nephelometer data were measured at a location somewhat removed from the flight tracks.

A complete analysis of the scattering as related to weather, wind patterns, and track locations relative to the city will not be attempted herein but will await the scientific report on the field trip. Also, at that time the data will be extrapolated to ground level.

The METRO scattering coefficient data show a much higher degree of variability over the 14-day period of the field trip than did the data for either of the previous two field trips, HAVEN VIEW and ATOM. All of the METRO flights have heavier haze at the lower altitudes than the ATOM flights. In comparison to the HAVEN VIEW haze at lower altitudes, the METRO haze measurements include flights having both heavier and lighter haze than HAVEN VIEW. Also, some of the METRO flights indicate a more complicated haze structure than the HAVEN VIEW flights.

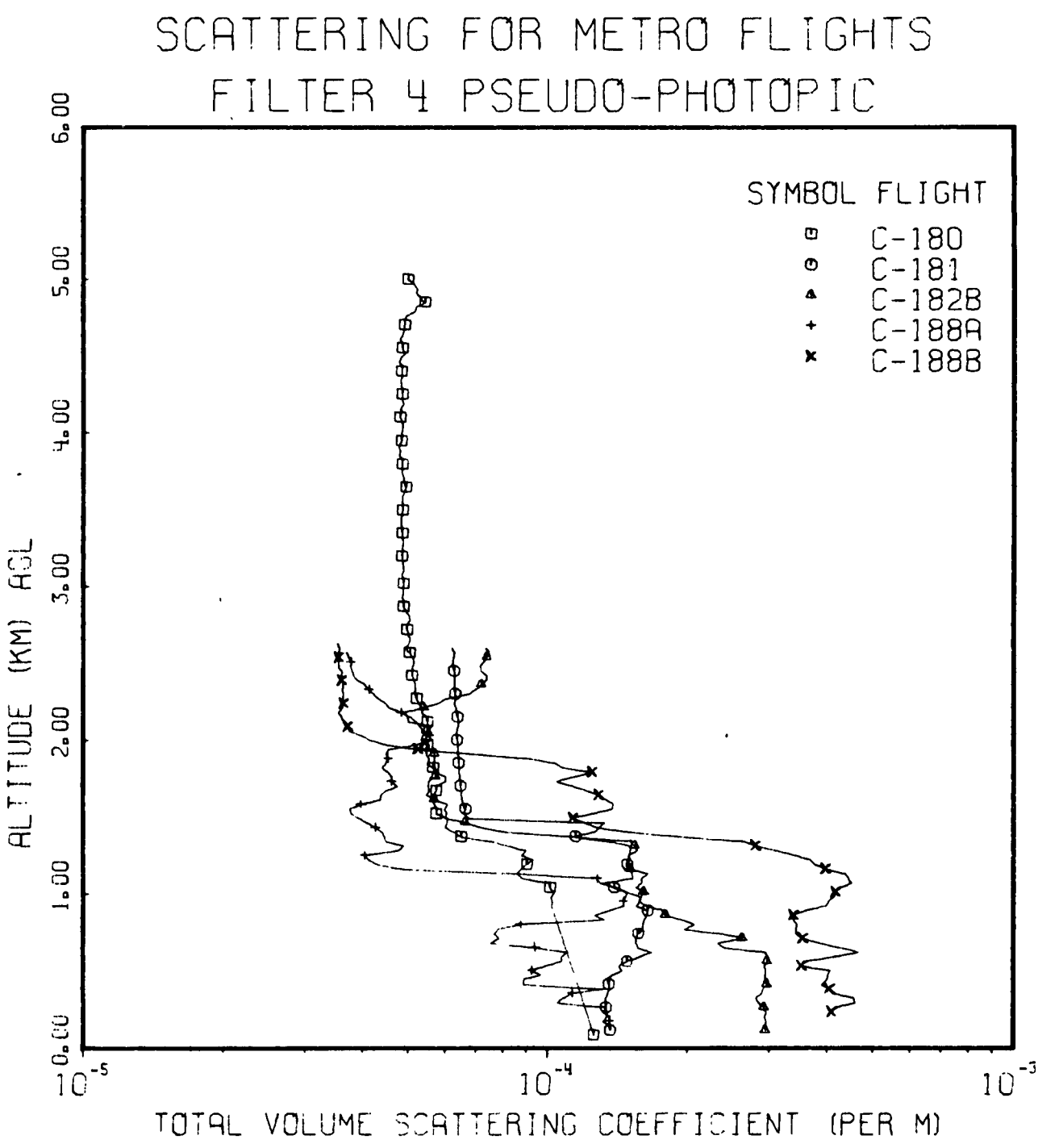

Fig. 7-6. Total Volume Scattering Coefficient for Filter 4 (Pseudo-Photopic) for Five METRO Flights, Flight Track 1, 3, 4, and 9.

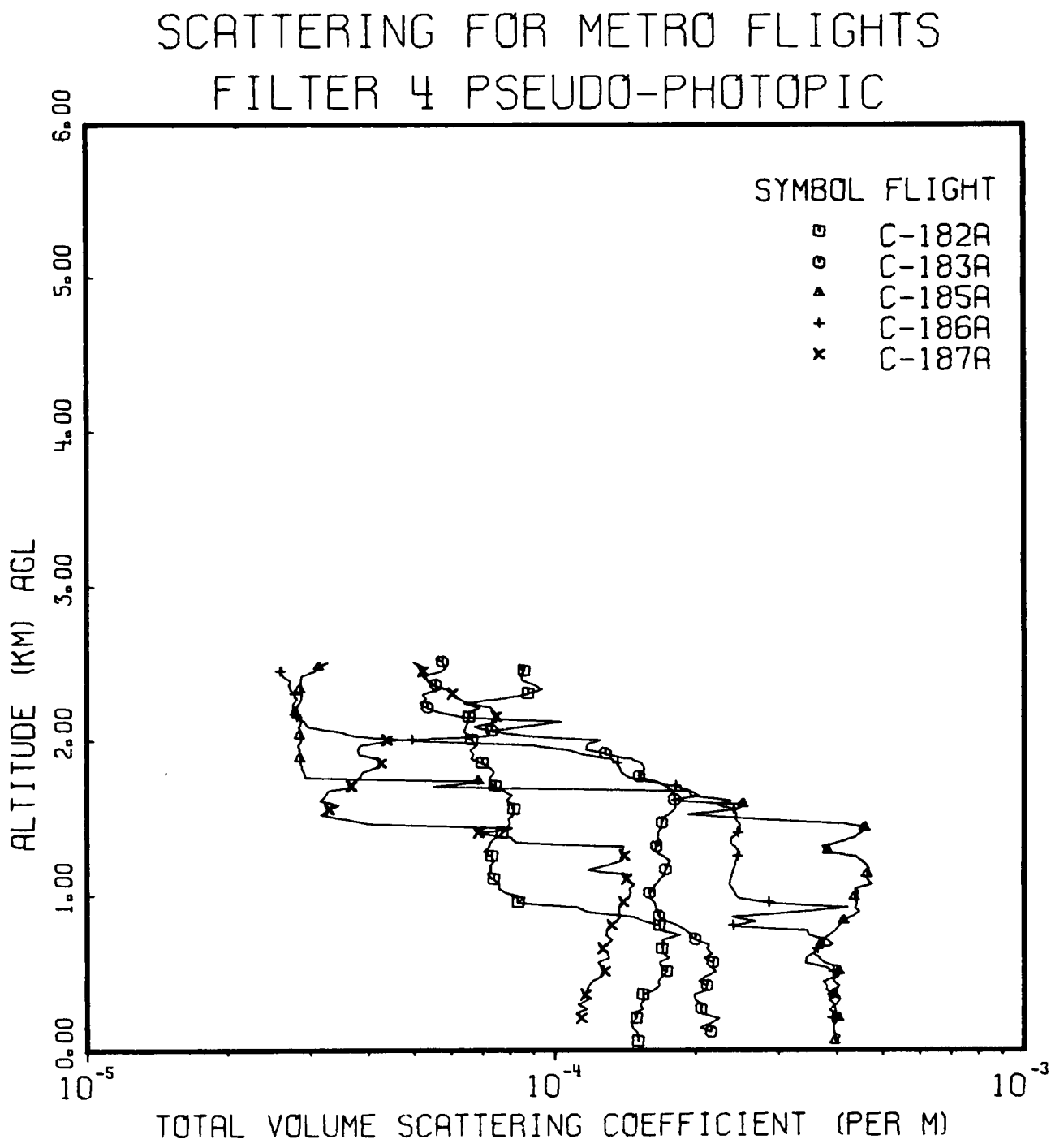

Fig. 7-7. Total Volume Scattering Coefficient for Filter 4 (Pseudo-Photopic) for Five METRO Flights, Flight Track 7.

Table 7-6

METRO Field Trip Data Summary

Flight No.	Date (1971)	Flight Track No.	Maximum Flight Altitude (meters) AGL	Total Time of Data-Taking	
				Start (GMT)	End (GMT)
C-180	11 August	1	5064	2033	0021
C-181	12 August	3	2627	1901	2040
C-182A	13 August	7	2490	1511	1640
C-182B	13 August	3	2615	1726	1856
C-183A	14 August	7	2550	1502	1635
C-185A	18 August	7	2550	1522	1700
C-186A	19 August	7	2520	1543	1707
C-187A	23 August	7	2520	1742	1900
C-188A	24 August	9	2580	1339	1501
C-188B	24 August	4	2643	1539	1658

Three of the METRO flights, C-185A, C-186A, and C-188B, show clearer high altitude data than either the ATOM or HAVEN VIEW flights. Two of the METRO flights, C-182A and C-182B, show less clear air at 2.5 kilometers than either the ATOM or HAVEN VIEW flights.

In the METRO data on Flight C-180, we again encounter, as in the HAVEN VIEW and ATOM data, a lapse rate at high altitude less than the density lapse rate. Since during the same field trip on Flight C-186A a total scattering coefficient measurement of 2.46E−5 was measured at 2.5 kilometers, which is half the value of the high altitude values for C-180, the nephelometer had clearly not reached a lower measurement limit for the C-180 measurements. This is presumptive evidence that the lapse rate measurements are valid.

8. PROJECTION AND RECOMMENDATIONS

As an outgrowth of the experience and expertise gained during the analysis and evaluation of the data gathered during this contract interval, several potentially powerful techniques have been devised. The improvement in overall analytic capability which will result from the implementation of these techniques is worthy of some further comment.

COMPOSITE SCANNER ARRAY

Many of the hardware and procedural modifications which were discussed or implied in Sections 3 and 4 were all related to one basic goal: the capability of generating a data array which completely and accurately portrays the spatial radiance distribution of the sky. The importance of having this array faithfully define radiance levels in the near sun regions cannot be overemphasized. Now that the operational capability is seemingly under control, the analytic exploitation of this data array should proceed. Even if there were no further development of computational procedures beyond the techniques discussed in Section 2 of Duntley, *et al.* (1972a and b), the utilization of this new composite data array would significantly improve the quality of the computed optical atmospheric properties. Fortunately, there are several additional gains to be derived from the existence of this new array. The most immediately attainable is an additional method for determining atmospheric beam transmittance.

BEAM TRANSMITTANCE DETERMINATIONS

The accurate determination of atmospheric beam transmittance is a necessary skill for any success in the field of atmospheric optics. During this contract interval there were only two techniques available for this determination. First, the airborne measurement of scattering coefficient profiles led to a computation of beam transmittances from the ground level up to altitudes of approximately 6 kilometers above ground level. These profiles could be extrapolated for earth to space, but with some moderate uncertainty attached to the extrapolation. Second, the ground-based measurement of apparent solar radiance would yield a computed value of earth-to-space beam transmittance, but with no clue as to the transmittance of intermediate path lengths.

A third technique is available if one has a reliable radiance array for the entire sky. The determination of atmospheric beam transmittance from the ratio of selected sky radiance values is described briefly in Section 2 of this report and also by Kushpil´ and Petrova (1971). This technique is currently

being developed at the Visibility Laboratory as an automatic process using computer techniques compatible with the general purpose routines illustrated in Fig. 5-1. Preliminary runs have been made using radiance arrays from Flight C-154, C-155, and C-157 with most encouraging results.

The application of this procedure to data arrays from more recent flights should be accomplished immediately. The technique is potentially powerful in that its application should be appropriate for data arrays measured at any altitude, including ground level, as well as data arrays measured during moonlight nights. The limitations imposed by the requirements for clear, cloudless skies and high instrumental precision do not seemingly outweigh the potential advantages of this additional computational tool.

SCATTERING FUNCTION RECOVERY

With the availability of a data set which contains reliable radiance gradient information near the sun, an improved computational technique for determining the atmospheric volume scattering function from these real-world measured data becomes increasingly attractive.

The proposed computational chain begins with the generation of the composite scanner data array, which provides the basic inputs for the subsequent steps. From this array a series of computations for beam transmittance is performed. These iterative computations make use of the basic ratio illustrated in Eq. (2.4) repeated below as Eq. (8.1) for the condition $\beta = \beta'$:

$$\frac{N^*_\infty(z,\theta,\phi)}{N^*_\infty(z,\theta',\phi')} = \frac{\bar{N}_q(\beta)[1 - T_\infty(z,\theta)]}{\bar{N}_q(\beta)[1 - T_\infty(z,\theta)]} \quad . \tag{8.1}$$

Once the atmospheric beam transmittance characteristics are fully and satisfactorily defined, the second link in the chain is prepared. In this step the sky radiance array and the computed values of beam transmittance are used to derive a set of equilibrium radiance values. This derivation makes use of Eq. (8.2) which is based upon Eq. (2.3):

$$\bar{N}_q(z,\theta,\phi) = \frac{N^*_\infty(z,\theta,\phi)}{[1 - T_\infty(z,\theta)]} \quad . \tag{8.2}$$

From these second link computations, an average effective equilibrium radiance function $\bar{N}_q(\beta)$ is generated for use in a variety of data array evaluations and adjustments prior to using the array for further computations. The procedure has been used on Flight C-154 data for debugging purposes, and up to this point in the chain, it is yielding impressively attractive results.

The third link in the chain is the most difficult and involves an attempt to recover the proportional directional scattering coefficient, $\sigma(\beta)/s$, from the $\bar{N}_q(\beta)$ function using Eq. (2.9). This procedure is currently under development at the Visibility Laboratory using available data arrays which at this point are of insufficient quality to yield fully satisfactory results. However, the technique appears profitable and worthy of intensive additional effort.

9. ACKNOWLEDGEMENTS

To be conducted successfully, a research program such as the one reported herein requires the active support of many organizations and individuals. To all of those who so willingly contributed their skills, talents, and inspiration, the authors gratefully acknowledge their debt.

Dr. Robert W. Fenn, Chief, Atmospheric Optics Branch, AFCRL,
Scientific Counsel and Technical Monitor
Major Leo J. Sheehan, USAF, Project Organization and Coordination
Mr. Raymond S. Silva, Operational Services Division, Field Requirements
Section AFCRL, for continuing logistical support and advice

3245th ABGp, L. G. Hanscom Field, for all aircrew assignments

Visibility Laboratory, Technical Field Team:

Mr. J. Douglas Bailey, ground station crew
Mr. George F. Simas, ground station crew
Mr. Leonard A. Castro, technical flight crew

Visibility Laboratory, Data Processing and Analysis Team:

Mr. Nils R. Persson, Jr.
Mrs. Janet E. Shields
Mrs. Catharine F. Edgerton
Miss Carolyn M. Williams

Visibility Laboratory, Editorial and Reproduction Team:

Miss Sally L. Poor
Mr. John C. Brown
Mrs. Arlene C. Streed
Mr. Louis S. Butler
Miss Alicia G. Enriquez

10. REFERENCES

Barteneva, O. D. (1960), "Scattering Functions of Light in the Atmospheric Boundary Layer," Bull. Acad. Sci. U.S.S.R., Geophysics Series, 1237–1244.

Brown, D. R. E. (1952), *Natural Illumination Charts*, Report 374-1, Project Ns-714-100, Department of the Navy, Bureau of Ships, Washington, D. C.

Buchtemann, W. and D. H. Hohn (1970), "Spectral Radiances of the Sky and Terrestrial Irradiance in the Wavelength Range from 0.38 to 0.84 μm," (Translation) Astronomisches Institut der Universität Tübingen.

Duntley, S. Q., A. R. Boileau, and R. W. Preisendorfer (1957), "Image Transmission by the Troposphere I," J. Opt. Soc. Am. **47**, 499-506.

Duntley, S. Q., R. W. Austin, J. L. Harris, and J. H. Taylor (1968), "Experiments on Visual Acuity and the Visibility of Markings on the Ground in Long Duration Earth-Orbital Space Flight," University of California, San Diego, Scripps Institution of Oceanography, Visibility Laboratory, SIO Ref. 68-6, also published by NASA, Washington, D. C., as NASA CR-1134 (1968).

Duntley, S. Q. (1969), "Directional Reflectance of Atmospheric Paths of Sight," Duntley Rep. No. 69-1.

Duntley, S. Q., R. W. Johnson, J. I. Gordon, and A. R. Boileau (1970), "Airborne Measurements of Optical Atmospheric Properties at Night," University of California, San Diego, Scripps Institution of Oceanography, Visibility Laboratory, SIO Ref. 70-7 and AFCRL-70-0137.

Duntley, S. Q., R. W. Johnson, and J. I. Gordon (1972a), "Airborne Measurements of Optical Atmospheric Properties in Southern Germany," University of California, San Diego, Scripps Institution of Oceanography, Visibility Laboratory, SIO Ref. 72-64 and AFCRL-72-0255.

Duntley, S. Q., R. W. Johnson, and J. I. Gordon (1972b), "Airborne and Ground-Based Measurements of Optical Atmospheric Properties in Central New Mexico," University of California, San Diego, Scripps Institution of Oceanography, Visibility Laboratory, SIO Ref. 72-71 and AFCRL-72-0461.

Gordon, J. I., J. L. Harris, and S. Q. Duntley (1963), "Earth-to-Space Contrast Transmittance Measurements from Ground Stations," University of California, San Diego, Scripps Institution of Oceanography, Visibility Laboratory, SIO Ref. 63-2.

Gordon, J. I. (1969), "Model for a Clear Atmosphere," J. Opt. Soc. Am. **59**, 14–18.

Gordon, J. I., J. L. Harris, Sr., and S. Q. Duntley (1972), "Method of Measuring Earth-to-Space Contrast Transmittance from Ground Stations," submitted to Applied Optics on 21 September 1972.

Kushpil', V. I. and L. F. Petrova (1971), "Determination of the Atmospheric Transmittance from Sky Brightness Distribution," Optical Technology **38**, No. 4, 191–193.

Tyler, J. E. and R. W. Preisendorfer (1962), "Light," Chap. 8 in *The Sea*, M. N. Hill, Ed. (Interscience Publishers, Inc., N.Y.), Vol. 1, pp. 397-451.

U. S. Standard Atmosphere (1962), U. S. Government Printing Office, Washington, D. C. 20402.

UNCLASSIFIED

Security Classification

DOCUMENT CONTROL DATA - R&D

(Security classification of title, body of abstract and indexing annotation must be entered when the overall report is classified)

1 ORIGINATING ACTIVITY (Corporate author)
University of California, San Diego
Visibility Laboratory
San Diego, California 92152

2a REPORT SECURITY CLASSIFICATION
UNCLASSIFIED

2b. GROUP

3 REPORT TITLE

AIRBORNE MEASUREMENTS OF OPTICAL ATMOSPHERIC PROPERTIES, SUMMARY AND REVIEW

4 DESCRIPTIVE NOTES (Type of report and inclusive dates)
Scientific, Final 1 November 1969 – 31 August 1972 Approved 1 November 1972

5 AUTHOR(S) (Last name, first name, initial)
Seibert Q. Duntley
Richard W. Johnson
Jacqueline I. Gordon

6 REPORT DATE	7a TOTAL NO OF PAGES	7b NO OF REFS
November 1972	79	15

8a. CONTRACT OR GRANT NO
F19628-70-C-0054

b. Project, Task, Work Unit No.
7621-04-01

c. DoD Element 62101F

d. DoD Subelement 681000

9a ORIGINATOR'S REPORT NUMBER(S)
SIO Ref. 72-82

9b OTHER REPORT NO(S) (Any other numbers that may be assigned this report)
AFCRL-72-0593

10 AVAILABILITY LIMITATION NOTICES

A – Approved for public release; distribution unlimited.

11 SUPPLEMENTARY NOTES
TECH, OTHER

12 SPONSORING MILITARY ACTIVITY
Air Force Cambridge Research Laboratories (OP)
L. G. Hanscom Field
Bedford, Massachusetts 01730

13 ABSTRACT

This report summarizes a 3-year period of collecting optical atmospheric data in the daytime chiefly with airborne instruments. Nine field expeditions were made between November 1969 and August 1972 in various places in the United States and Europe, primarily during the spring and fall. Measurements were made in five spectral regions, as follows: three narrow band optical filters with mean wavelengths of 478, 664, and 765 nanometers, and two broad band sensitivities, one representing the S-20 multiplier phototube incorporating an ultraviolet rejection filter with a mean wavelength of 532 nanometers, the other representing the photopic response with a mean wavelength of 557 nanometers. Optical measurements included total scattering coefficient and sky and terrain radiance. These data were used to calculate natural irradiance on a horizontal plane surface, directional reflectance of terrain, atmospheric beam transmittance, path radiance, and directional path reflectance. The methods of data collection and data processing are reviewed, the resultant data bank described, and initial comparisons made between several of the field expeditions.

DD FORM 1 JAN 64 1473

UNCLASSIFIED

Security Classification

14 KEY WORDS	LINK A		LINK B		LINK C	
	ROLE	WT	ROLE		ROLE	WT
Atmospheric Optical Properties						
Atmospheric Scattering Coefficient						
Atmospheric Beam Transmittance						
Atmospheric Contrast Transmittance						
Atmospheric Path Reflectance						
Daytime Radiance						
Daytime Irradiance						
Terrain Reflectance						
Radiometry						